Arabian Journal of Geosciences (2022) 15:317
https://doi.org/10.1007/s12517-021-09180-y

REVIEW PAPER

Oceanic anoxic events in the Earth's geological history and signature of such event in the Paleocene-Eocene Himalayan foreland basin sediment records of NW Himalaya, India

Bhart Singh[1] · Seema Singh[1] · Uday Bhan[2]

Received: 13 October 2021 / Accepted: 30 November 2021

Abstract

Oceanic anoxic events (OAEs) represent changes in global carbon cycle as well as biogeochemical cycles and are robust recorders of major changes brought in the ocean-atmosphere system of the Earth. In the present study, a comprehensive compilation of well-documented OAEs in the Earth's geological history indicates that compared to the plethora of OAE studies in different parts of the world, the Indian part lacks sufficient such geological studies. Also, it has been observed that despite the variety of causes referred by researchers for the occurrence of OAEs based on various geological proxies, their development tends to cluster in particular periods having unique geological settings under specific climate conditions of the Earth. OAEs usually coincided with Earth's greenhouse condition and in marine to shallow marine depositional settings, which have been associated with rapid alternating phases of transgression and regression. The Paleocene-Eocene thermal maximum (PETM) at the Paleocene-Eocene boundary comprises the last OAE of the Phanerozoic Eon and the only identified OAE in the Cenozoic. The deposition of Himalayan foreland basin sediments during Paleocene-Eocene time coincides with the India-Eurasia collision and PETM. Characteristic litho sections of Paleocene-Eocene HFB shallow marine sediments represented by the Subathu Formation occur in and around the Jammu region (of the Ramngar sub-basin) and Simla region (of the Subathu sub-basin) of NW Himalaya (India) and have been explored for OAE records. Besides the fact that deposition of these sediments coincides with PETM, there are many other reasons which suggest possible representation of these as records of OAE. For example, these sediments show OAE specific sedimentary and biostratigraphic facies associations which are characteristic of alternating transgressive-regressive successions. The base of these early HFB sediments consists of sideritic ironstone, phosphorite, and black shale association indicating commencement of basinal sedimentation under euxinic, shallow marine conditions. Though these Paleocene-Eocene HFB sediments comprising dominantly black to gray-green shales are regionally extensive, however, these occur in discontinuous patches all along the HFB and also greatly vary in thickness due to the tectonic complexity of the Himalayan region.

Keywords Oceanic anoxic events (OAEs) · Himalayan foreland basin (HFB) sediments · Paleocene-Eocene thermal maximum (PETM) · Subathu formation · Himalayan orogeny

Introduction

The Earth's geological history had been interrupted by major geological events. This is well documented on the basis of multi-proxy data and evidence. OAEs/anoxic events represent one such signature. The anoxic event refers to the time interval when portions of oceans become depleted in oxygen over a significantly large geographic area (Schlanger and Jenkyns 1976; Jenkyns et al. 2004; Jenkyns 2010; Jenkyns et al. 2017). These were first described in detail by Schlanger and Jenkyns (1976) from the discoveries made by the deep-sea drilling project in the Pacific Ocean. In general, multiple

Responsible Editor: Attila Ciner

✉ Seema Singh
geoseema05@yahoo.co.in

[1] Department of Geology, Panjab University, Chandigarh 160014, India

[2] Department of Petroleum Engineering and Earth Sciences, University of Petroleum and Energy Studies, Dehradun 248007, India

Published online: 03 February 2022

geological records have shown that the anoxic events though were not continuous for millions of years but occurred many times as short time span intervals in the Earth's geological history (Fig. 1). There has been significant research work done across the world, wherein it has been shown that OAEs are robust recorders of past global changes in Earth's climate and ocean chemistry bringing out major changes in the global carbon cycle (Jenkyns 2010; Jenkyns et al. 2017). Also, researchers have temporally associated these with large igneous provinces ((LIP) Mukherjee et al. 2017) as well as mass extinction events (Ernst and Youbi 2017; Bastos et al. 2020; Kabanov and Jiang 2020; Kuroyanagi et al. 2020; Hennekam et al. 2020; Fig. 1).

The OAEs are primarily defined by the relatively high total organic content (TOC) level and are associated with a perturbation in the global carbon cycle, but the forcing mechanism behind this is still debatable. Researchers have documented the occurrence of OAEs worldwide at different times (Table 1) and suggested many factors either alone or in combination which are responsible for bringing changes in eustatic level, tectonism, volcanism, dissolution of gas hydrates, oceanic circulation pattern as well as asteroid impacts (Schlanger and Jenkyns 1976; Jenkyns et al. 2004; Jenkyns 2010; Pandey and Pathak 2016 and references therein; Jenkyns et al. 2017; Jenkyns 2018; Kemp et al. 2020; Bonacina et al. 2021). For example, these factors could become a cause for the abrupt rise in global temperature accompanied by accelerated hydrological cycle, increased continental weathering, enhanced nutrients discharge into the ocean and lakes, intensified upwelling, and increase in organic productivity (Schlanger and Jenkyns 1976; Arthur and Sageman 1994; Larson and Erba 1999; Leckie et al. 2002; Weissert and Erba 2004; Jenkyns 2010; Jenkyns et al. 2017; Kemp et al. 2020; Bonacina et al. 2021).

A distinguishing feature of OAEs is that they are characterized globally by exceptionally high rates of organic carbon burial in sediments ranging from deep-ocean to shallow water marginal seas. Thus, they are conspicuously represented by sedimentary facies comprising organic rich, dominantly dark gray to black shale facies. Since the sediments are organic rich, it indicates either greater preservation of organic matter or increased rate of organic influx versus oxygen availability in seawater column (Arthur and Sageman 1994 and references therein; Brumsack 2006 and references therein). Their short time intervals show unusually increased rates of organic carbon burial (1–30%). Such sediments characteristic of anoxic events is favorable source rocks for hydrocarbon reserves. Researchers have shown that more than 50% of the known petroleum deposits worldwide comprise source rocks in sediments/lithofacies deposited during anoxic events (Arthur and Schlanger 1979; Klemme and Ulmishek 1991; Sageman 2006 and references therein; Soua and Chihi 2014; Soua 2016; Pandey and Pathak 2016; Talbi et al. 2019 and references therein Kassem et al. 2020; Wentong He et al. 2021 and many more). Sageman (2006) documented that these

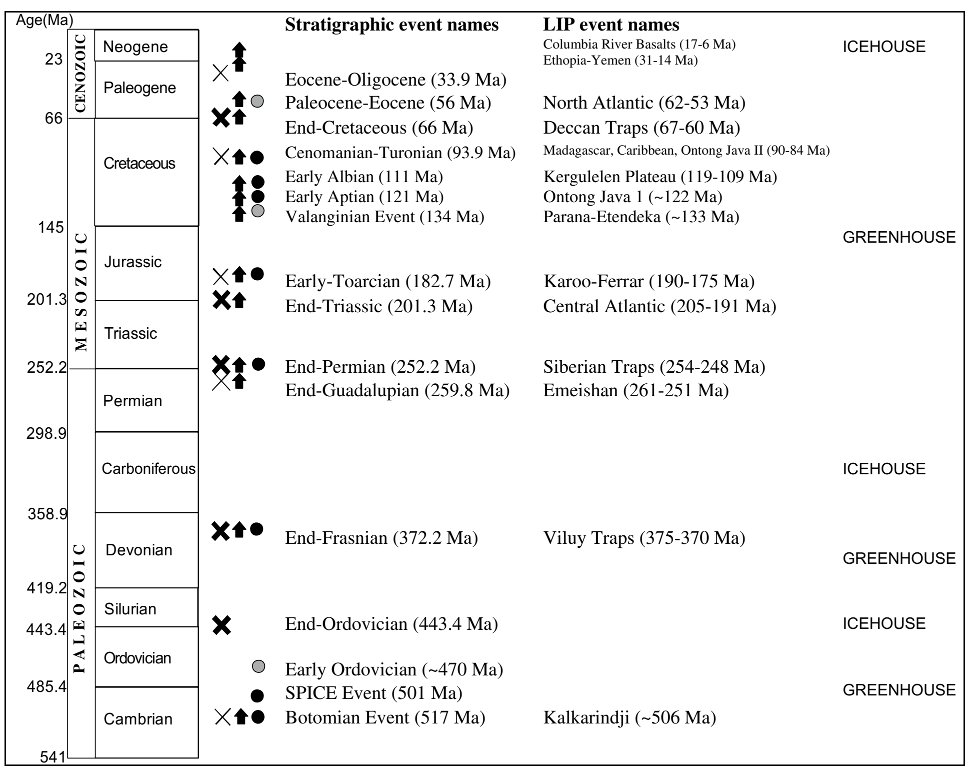

Fig. 1 An illustration as shown by Percival et al. (2015), wherein temporal correlation of LIPs with OAEs and/or extinction events has been shown during Phanerozoic history of Earth. Symbols key: arrow represents LIP, filled circle represents OAE, bold cross represents major mass extinction and normal cross represents minor mass extinction (for details refer to Percival et al. 2015 and references therein)

Table 1 Compilation of locations wherein researchers have identified OAEs in the Cenozoic, Mesozoic, and Paleozoic Era

Era	Geologic time (age in Ma)	Reference for details *(location/section)*
Cenozoic	Middle Miocene (15.6–16)	Kidder and Worsley 2010 *(Columbia River Basalt)*
	Early Oligocene (29–31)	Kidder and Worsley 2010 *(Ethiopian Highlands)*
	Oligocene–Miocene (39–23)	Kokh et al. 2021 *(Kerch Peninsula, Ukraine)*
	Toarcian OAE (183)	Suan et al. 2008 (Lusitanian basin, Portugal); Gröcke et al., 2011 *(Toyora area, Japan)*; Izumi et al. 2012 *(Yorkshire)*; French et al. 2014 *(Yorkshire, Germany, Italy)*; Huang and Hesselbo 2014 *(Andean Basin, Chile, South-America)*; Fantasia et al. 2018 *(Sakuragu-chi-dani section, Japan)*; Kemp et al. 2020 *(Trans-danubian Range, Hungary)*; Főzy et al., 2010 *(Vocontian Basin, France)*; Duchamp-Alphonse et al. 2011 *(Italy)*; Arora et al. 2015 *(Juran Formation, India)*
Mesozoic	Late Valanginian OAE (136.4)	Najarro et al. 2011 *(North Spain)*; Moiroud et al. 2012 *(Baltic Cordillera, SE Spain)*; Bottini et al., 2012 *(Southern Alps, New Zealand)*
	The Hauterivian OAE (130)	Kuypers et al., 2002 *(North Atlantic Ocean off the coast of Florida and the Ravel section of the Southeast France)*; Khan et al. 2021 *(Mughal kot section, Pakistan)*; Coccioni et al. 2012 *(Poggio le Guaine section Umbria-mache basin, Italy)*
	Early Aptian OAE 1a (120)	Li et al. 2016 *(Southern Tibet, China)*; Karakitsios et al. 2010 *(Greece)*; Bastos et al. 2020 *(N-E Brazilian basin, Brazil)*, Sanchez-Hernandez and Maurrasse 2016 *(Organya basin spain)*; Li et al. 2008 *(Cismon Apticore in Italy, Santa Rosa Canyon in north-eastern Mexico, and Deep Sea Drilling Project Site 398)* Matsumoto et al. 2020 *(Poggio le Guaine, PLG, record, central Italy and Spain)*
	Early Albian OAE 1b (112)	Mort et al. 2007 *(Italy and Spain)*; Kellar et al. 2008 *(Tarfaya Basin of Morocco)*; Tsiko et al. 2004 *(Eastbourne, England, Gubbio, Italy, Tarfaya, Morocco)*; Tiwari et al. 1996, Nagendra and Reddy 2017, Bansal et al. 2018 *(Cauvery basin, India)*
	Cenomanian-Turonian OAE (99.6–93.5)	Wang et al. 2001 *(Southern Tibet)*; Kassem et al. 2020 *(Central Gulf of Surez, Egypt)*; Bomou et al. 2013 *(Tibet)*; Voigt et al. 2008 *(Wunstorf section, North Germany)*; Duque-Botero et al. 2009 *(Indidura Formation, Mexico, Furlo in the Marche–Umbrian Apennines of Italy)*; Owens et al. 2017, Lenniger et al. 2014 *(Axel Heiberg Island, Canada)*; Al-Sagri, 2015 *(Gulneri Formation, Northern Iraq)*; Jenkyns 2018 *(Cismon, North Italy, South Provence Basin, Southeast France Iberian Margin, Site 39)*; Keller et al., 2021 *(Western Narmada basin, India)*
	Coniacian Santonian (93.5)	Sachse et al. 2012 *(Tarfaya Basin, Morocco)*; Andjic et al. 2018 *(Loma Chumico Formation of N-Costa Rica)*; *(Tunisia, Africa)*; Heath et al. 2021 *(English river formation, Illinois, US)*
Paleozoic	Devonian (419.2–358.9)	Buggisch, 1991b*(France, Australia)*; Kabanov 2019 *(Mackenzie platform, Canada)*; Langsford 2020 *(South Australia)*
	Carboniferous (358.9–323.2)	Cheng et al. 2020 *(Nevada, USA)*

black shale deposits store quantities of carbon sufficient to source all of the petroleum and natural gas that humans have thus far consumed or will ever produce. Further, Soua and Chihi (2014) described a new method for exploration procedure which is based on the knowledge of OAEs distribution maps so as to identify main source rocks existence to improve understanding of new petroleum systems.

The OAEs are restricted to certain geologic time periods (Fig. 1). Both global and regional OAEs have been recognized by a number of researchers to specific chronostratigraphic intervals. Amongst all, the most commonly discussed OAEs fall during the Mesozoic Era, particularly comprising the Jurassic-Cretaceous span (Jenkyns 2010 and Arora et al. 2015; Fig. 2). Buggisch (1991a) documented in detail such OAEs during the Paleozoic Era which in particular falls during the Devonian Period. Jenkyns (2010) established that the PETM at the Paleocene-Eocene boundary (i.e., ~55 Ma), perhaps comprises the last OAE of the Phanerozoic Eon (Fig. 2).

The major OAEs have been studied extensively in parts of Europe, Africa, USA, Argentina, SE China, Japan (Tsikos et al. 2004; Hu et al. 2014; Millán et al. 2014; Richiano 2014; Soua 2014; Percival et al. 2015, 2020; Boulila and Hinnov 2017; Jenkyns et al. 2017; Valle et al. 2019; Kemp et al. 2020; Joo et al. 2020; Bonacina et al. 2021; Table 1; Fig. 3). In India, the Mesozoic of Spiti valley comprising Jurassic-Cretaceous succession need better investigations for OAEs (Arora et al. 2015) compared to similar chronostratigraphic equivalents in the Kutch (Arora et al. 2015; Biswas 1977), Narmada basin (Keller et al. 2021), and Cauvery basins (Sundaram et al. 2001; Krishna 2017; Nagendra and Reddy 2017; Bansal et al. 2019). On the contrary, detailed studies for investigating such global and/or regional OAEs are meager in the Paleozoic (i.e., Devonian) and early

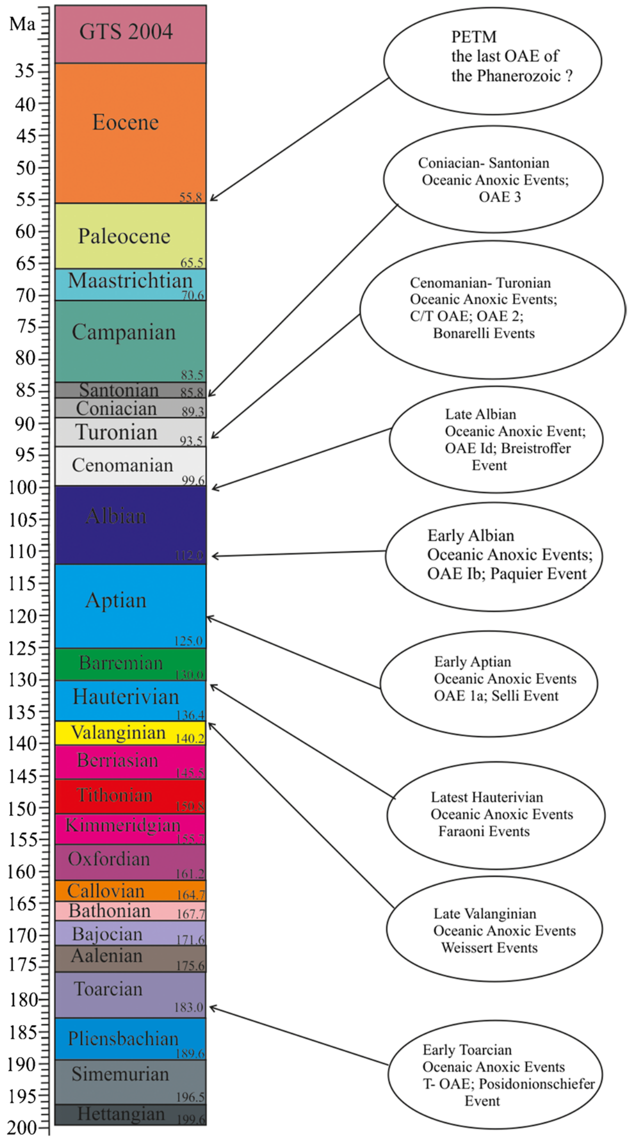

Fig. 2 Various oceanic anoxic events during the Mesozoic and Cenozoic times in the geological history of Earth as compiled by Jenkyns (2010)

Cenozoic (i.e., Paleocene-Eocene) lithostratigraphic units of the Indian part of geology irrespective of reports of these coeval events in other parts of the world (Jenkyns 1999, 2010; Leckie et al. 2002; Erba, 2004, b). Thus, compared to the plethora of such geological studies in other parts of the world, the Indian part lacks sufficient studies, thereby requiring investigation of coeval, globally established OAEs.

The major objective of this study is the comprehensive compilation of well-recorded global OAEs to understand the possibility of occurrence of an anoxic event during deposition of earliest Himalayan foreland basin sediments (i.e., final closure of Tethys Sea during Paleocene-Eocene) coeval with PETM. An overall compilation of various documented factors which specifically led to well-established global OAEs in different times has been briefly discussed for a holistic appraisal of possibilities of any record of these events in the NW Himalaya (India) during PETM. This review article wherein temporal and spatial scale compilation of past oceanic anoxic events and factors responsible for this will further allow us to think toward the role of local to regional/global factors responsible for anoxic conditions. Such reviews are critical since numerous geological records show close association of global scale OAEs with mass extinctions and the recent time oxygen-deficient conditions in the marine system require the need to explore past such events. As an example, Hennekam et al. (2020) suggested the significance to search for statistical indicators/early-warning signals that can be probed for the future transition of a marine system into fast deoxygenation. They demonstrated this by analyzing past widespread anoxic events from sedimentary archives in the eastern Mediterranean Sea, wherein regular rapid oxic-to-anoxic transitions occurred on (multi) centennial time scales.

Characteristics of oceanic anoxic events (OAEs)

Sedimentary characteristics

Sedimentologically, the OAEs are strongly characterized by the presence of gray, dark green to black colored, fine sediments commonly shale facies as has been documented by a significant number of researchers and comprise alternating typical transgressive and regressive sedimentary facies. The sediments are commonly organic rich and laminated. The other common sedimentary features observed within this clastic-dominated sedimentary interval are current ripple and hummocky cross stratifications (Krencker et al., 2019).

The presence of organic carbon is considered to be the basic material required for the occurrence of oceanic anoxic events as demonstrated by Tsikos et al. (2004) in the evident Cenomanian-Turonian OAE outcrop located near Gubbio in the Marche-Umbrain Apennine of central Italy. The early Toarcian transgression (T-OAE) is marked by the occurrence of organic-rich shale in large parts of Western Europe as well as in other parts of the world (Sabatino et al. 2009). For example, the widespread occurrence of early Toarcian shale has been interpreted to be deposited during the global OAE, particularly on evidence of positive stable carbon isotope excursions from pelagic limestone sediments in several Tethyan studied sections (Jenkyns 1988; Jenkyns and Clayton 1997; Jenkyns, 1999, 2010, 2017). The rapid burial of the large amount of organic carbon which is rich in carbon-12 would have led to a relative enrichment in δ^{13}C of the global carbon reservoir and hence an increase in δ^{13}C of limestone.

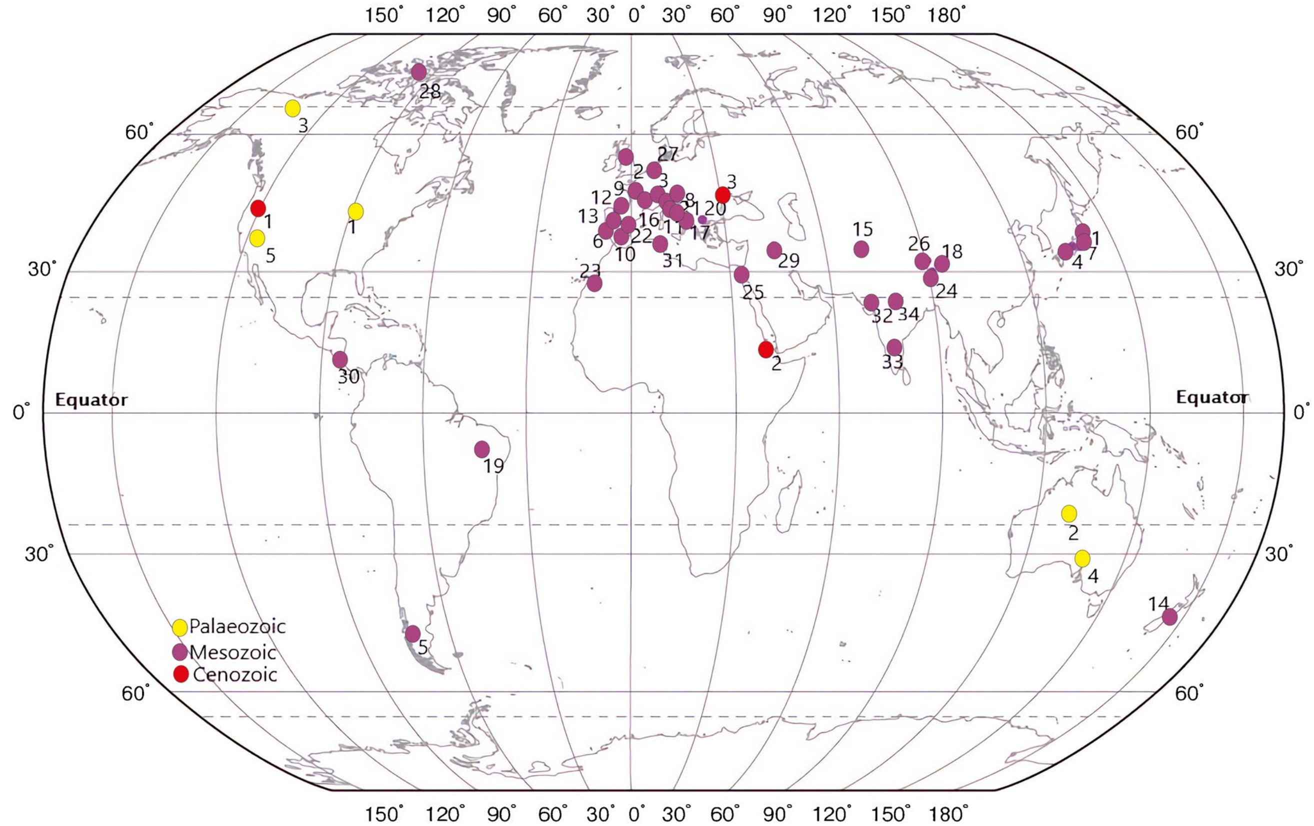

Fig. 3 Representation of various OAEs in the world as documented by researchers. PALAEOZOIC: 1. English river Formation, Illinois, US (Heath et al. 2021); 2. Australia (Buggisch, 1991a); 3. NW Canada (Kabanov 2019); 4. South Australia (Langsford 2020); 5. Nevada, USA (Cheng et al. 2020). MESOZOIC: 1. Sakuraguchi- dani section, Japan (Kemp et al. 2020); 2. Yorkshire (French et al. 2014); 3. Yorkshire, Germany, Italy (Huang and Hesselbo 2014); 4. Toyora area, Japan (Izumi et al. 2012); 5. Andean Basin (Chile), South-America (Fantasia et al. 2018); 6. Lusitanian basin, Portugal (Suan et al. 2008; Duque-Botero et al. 2009); 7. Japan (Gröcke et al., 2011); 8. Transdanubian range, Hungary (Fozy et al., 2010); 9. Vocontian Basin, SE France (Duchamp-Alphonse et al. 2011); 10. Beltic Cordillera, SE Spain (Moiroud et al. 2012); 11. Italy (Li et al. 2008; Tsiko et al. 2004); 12. North Spain (Najarro et al. 2011); 13. South central, Spain (Sanchez-Hernandez and Florentin, 2016); 14. Southern Alps, New Zealand (Bottini et al., 2012); 15. Mughal kot section, Pakistan (Khan et al. 2021); 16. Southeast France (Kuypers et al., 2002; Owens et al. 2017; Jenkyns 2018); 17. Central Italy; 18. Eastern Tethys, Southern Tibet, China (Li et al. 2016); 19. North-eastern Brazilian basins, Brazil (Bastos et al. 2020); 20. Greece (Karakitsios et al. 2010); 21. Central Italy (Matsumoto et al. 2020); 22. Italy and Spain (Mort et al. 2007); 23. Tarfaya Basin, Morocco (Kellar et al. 2008; Sachse et al. 2012); 24. Southern Tibet (Wang et al. 2001); 25. Central Gulf of Surez, Egypt (Kassem et al. 2020); 26. Tibet (Bomou et al. 2013); 27. Wunstorf section, North Germany (Voigt et al. 2008); 28. Axel Heiberg Island, Canada (Lenniger et al. 2014); 29. Gulneri Formation, Northern Iraq (Al-Sagri, 2015); 30. Loma Chumico Formation, N-Costa Rica (Andjic et al. 2018); 31. Tunisia, Africa. CENOZOIC: 1. Columbia River Basalt (Kidder and Worsley 2010); 2. Ethiopian Highlands (Kidder and Worsley 2010); 3. Kerch Peninsula, Ukraine (Kokh et al. 2021)

The three major OAEs in the Mesozoic have been studied in detail (Jenkyns 1999, Fig. 2) and are marked by similar sedimentary facies at the global scale, comprising pelagic black shales confined within a biostratigraphic interval of 1Ma or less (Schlanger and Jenkyns 1976; Weissert 1989; Jenkyns and Clayton 1997; Jenkyns, 1999, 2010 and many more). However, OAEs can show varied sedimentary facies record at local scales, having sediments completely lacking organic matter indicating that the favorable condition for the same could be simply increased organic productivity by whatever means (Jenkyns 2010 and references therein).

Likewise, though a number of OAEs have been reported from the Cretaceous successions of the Mesozoic, only one such definitive global OAE has been reported from the Early Jurassic Period of the Mesozoic Era which is named as Toarcian OAE, i.e., T-OAE (Schlanger and Jenkyns 1976; Coccioni et al. 1987; Jenkyns 1988, 2010; Hesselbo et al. 2000, 2007; Leckie et al. 2002; Baudin 2005; Cohen et al. 2007; Pearce et al. 2008; Nozaki et al. 2012; Satpathy et al. 2013; Arora et al. 2015 and references therein). In general, the sedimentary record of the most common global T-OAE is characterized by organic-rich sediments, dominantly black shale associated with a distinctive negative excursion in $\delta^{13}C$

values as has been observed in various early Jurassic dated sections (Jenkyns and Clayton 1997; Cohen et al. 2004; Hesselbo et al. 2007; Suan et al., 2008; Hermoso et al. 2009; Bodin et al. 2010).

In recent years, much has been done to improve our understanding of the black shale deposition in a sedimentary environment. The nature of black shale also depends upon the basin evolution and paleogeography. The spatial and temporal distribution of black shale is linked to the development of the environment in which they accumulate and to the propitious combination of environment variables. Various researchers have shown that the deposition of black shales associated with OAEs varies from shallow to deep marine environments. Presence of such abundant black shales at the global scale and restricted within short span chronostratigraphic intervals have been documented largely from the Mesozoic strata by a wide array of researchers (Jenkyns 2010, 2018 and references therein; Nozaki et al. 2012, Phelps et al. 2015; Boulila and Hinnov 2017; Jenkyns et al. 2017; Joo et al. 2020; Kemp et al. 2020; Uveges et al. 2020; Bonacina et al. 2021 and references therein).

Geochemical characteristics

The geochemical characteristics can be interpreted by TOC value, hydrogen index (HI), oxygen index (OI), biomarkers (derived from different strains of green Sulfur bacteria), major and trace elements. Besides the carbon stable isotope signatures, oxygen and nitrogen isotope ratios as well as Mg/Ca values show specific variation/trend during these OAE. For example, Higgins et al. (2012) demonstrated that the OAE 2 shales of the Mesozoic Era was characterized by low nitrogen isotope ratio, values varying between −4 and 2 ‰ than the modern marine setting shales and thus can be used as a geochemical indicator of the occurrence of OAEs during Mesozoic. This could be because of the development of oxygen minimum zones during Cenomanian–Turonian, Aptian, and T-OAE which ultimately led to the total depletion of nitrogen (Ohkouchi et al. 1997, 2006; Farrimond et al. 2004; Kuypers et al. 2004; Dumitrescu and Brassell 2006, Jenkyns, 2010).

Phosphorus element variation in marine sediments has also been documented as an indicator of OAEs. Most of the phosphorus that reaches the seafloor arrives in the form of organic matter accumulations. Phosphorus (P) in buried in three main forms namely, organic-P, Ca-P, and Fe-P. It has been demonstrated that under anoxic bottom water the burial of organic-P and Fe-P is suppressed (Ingall et al. 1993; Van Cappellen and Ingall 1994; Colman et al. 1997; Colman and Holland 2000). The ratio of carbon (C) and phosphorus (P) is buried organic matter (C/P) organic is equivalent to 4000 for laminated black shale deposited under anoxic conditions, but only around 150 for bioturbated shale deposited under oxic conditions (Ingall et al. 1993). The evidence in these intervals of C/T OAE 2 suggests its global nature. Thus, to conclude there is a decline in the efficiency of phosphorus during anoxic conditions and vice versa. The recycling of phosphorus from the bottom water further enhances the planktonic activity (Van Cappellen and Ingall 1994, Mort et al. 2007; Jenkyns, 2010; Beil et al. 2020; Percival et al. 2020). Increased TOC/P_{TOT} ratio in the Frasnian-Famennian lower and upper Famennian Annulata and Hangenber level suggest that such nutrient recycling occurred across the area of the marine shelf in Laurentia and Rheic ocean margin during those times which helped to sustain reducing conditions in those environments. Elevated P_{TOT} values in the upper Kellwasser, Annulata, and Hagerberg levels are consistent with an enhanced nutrient influx as the initial trigger for Anoxia (Percival et al. 2020; S.beil et al. 2020).

Trace elements V, U, Ni, and Mo are sensitive to the redox environment and their ratios (Arthur and Sageman 1994; Morford and Emerson 1999; Fleurance et al. 2013). For example, U/Th, V/Cr, Ni/Co, and V/V + Ni have been used for the interpretation of paleo-redox conditions (Algeo and Maynard 2004; Pi et al. 2013). Their values are used to distinguish oxic, dysoxic, and anoxic grades. However, their ratios do not show good correlations with TOC content because oxic and dysoxic conditions are unfavorable for organic matter preservations. The geochemical interpretations from ancient black shale are often complicated because of the post-depositional modifications by deep burial processes. Nevertheless, geochemical studies of black shale sedimentary successions are significant to understand the cause and consequence of enhanced organic matter burial.

Decades of research has been carried out on stable carbon isotope ratios in order to understand any trend in its variation due to sudden perturbations of the carbon cycle during OAE (e.g., Arthur et al. 1985; Pratt 1985; Arthur et al. 1987; Stoll and Schrag 2000; Tsikos et al. 2004; Erbacher et al. 2005; Gale et al. 2005; Jarvis et al. 2006; Li et al. 2006; Sageman et al. 2006; Wendler et al. 2009; Barclay et al. 2010; Takashima et al. 2011; Jarvis et al. 2011; Eldrett et al. 2014; Joo and Sageman 2014; Jenkyns et al. 2017). In general, such isotopic data can be used as a multi-proxy geochemical tool, as a proxy for reconstructing changes in the mass balance of the global carbon cycle, and as a chronostratigraphic tool. Adopting $\delta^{13}C$ datasets as a means of tracking changes in the carbon cycle, changing atmospheric CO_2 levels and climate, previous studies by Freeman and Hayes (1992), Hasegawa (2003), Jarvis et al. (2011), and others, during the Late Cenomanian compared stable carbon isotope composition of carbonates with marine organic matter and/or terrestrial woody material because the enormous increase in carbon burial is expected during an OAE. The carbon isotope signatures of early Albian, early Aptian, and early Toarcian are confusing because the sediments show both negative and positive isotope excursions (Jenkyns and Clayton 1986, 1997; Menegatti et al. 1998; Schouten et al. 2000; Jenkyns 2003; Herrle et al., 2004). In the C/T OAE 2, all sections demonstrate a subdued negative shift within the broad positive carbon isotope excursion which is particularly pronounced in the organic carbon isotope record at the base of the Livello Bonarelli section where a fall of 3‰ has been observed (Kuroda et al., 2007). Thus, addition of some isotopically light carbon isotope happened into the ocean–atmosphere system during the C/T OAE. Researchers documented that the possible reasons for this could have been volcanism or dissociation of gas hydrates or thermal metamorphism of coal either alone or in combination (Hesselbo et al. 2000; Jahren et al. 2001; Jenkyns 2003; Jenkyns, 2010; McElwain et al. 2005; Kuroda et al., 2007).

Stable oxygen isotope studies from the bulk and skeleton samples corroborate its connection with the relative thermal maxima. In Cenomanian-Turonian, the oxygen isotopic data from the north European American chalk and well-preserved brachiopods suggests a rise in temperature of 6–7 °C during late Cenomanian and mid-Turonian (Jenkyns, 2010; Voigt et al. 2006). The oxygen isotope data from the well-preserved foraminifera in the equatorial Atlantic show temperature fluctuations of 4 °C during C/TOAE (Forster et al. 2007). Likewise, such a trend has been documented in the Albian Paquier black shale at its type locality where the temperature rose up to 8 °C (Herrle et al. 2003). The oxygen isotope data from deep-sea drilling cores similarly suggest abrupt warming intervals represented by the base of the black shale which was followed by cooling intervals (Erbacher et al. 2001). Therefore, various compilations indicated that during Toarcian oxygen-18 isotope had minimal value and temperature records have been around 6–7 °C (Bailey et al. 2003).

Spatial and temporal distribution

Early in the 1970s, multiple organic-rich sediments, dominantly of black shales have been identified during the execution of Deep Sea Drilling Projects (DSDP) on Tethyan Mesozoic deep-sea sediments to the North Atlantic Ocean (Bernoulli 1972). Later Schlanger and Jenkyns (1976) first identified the worldwide occurrence of similar black shales in different sedimentary basins which could have been possible due to the occurrence of synchronous global events. It was further observed that these organic-rich sediments were confined to short intervals of time. This led Schlanger and Jenkyns (1976) to first coin the term OAE which has been defined as short-spanned episodes in the Earth's history, characterized by the presence of organic-rich sediments deposited under dysoxic to anoxic conditions.

Within a short span of time, researchers identified a number of these anoxic events in the Earth's geological history in different parts of the world, thereby resulting in significant advances in fields of palaeoclimatology, palaeoecology, palaeoceanography, palaeontology, and sedimentology (Table 1; Fig. 3; Arthur and Schlanger 1979; Demaison and Moore 1980; Jenkyns 1980, 1988; Biswas 1981; Arthur et al. 1990;Buggisch, 1991a; Arthur and Sageman, 1994, 2005; Bhargava and Bassi 1998; Srikantia and Bhargava 1998; Jenkyns 1999, 2003, 2010, 2017; Krishna et al. 2000; Bottjer et al. 2001; Huber et al. 2002; Leckie et al. 2002; Erba et al., 2004; Tsikos et al. 2004; Bertle and Suttner 2005; Takashima et al. 2006; Banerjee et al. 2006; Hesselbo et al. 2007; Al-Suwaidi et al. 2010; Najarro et al. 2011; Pathak et al. 2011; Bottini and Mutterlose 2012; Lehmann et al. 2012; Pandey et al. 2013; Hu et al. 2014; Millán et al., 2014; Richiano 2014; Soua 2014; Godet et al. 2014; Arora et al. 2015; Percival et al. 2015, 2020; Boulila and Hinnov 2017; Jenkyns et al. 2017; Joo et al. 2020; Bastos et al. 2020; Kavanov et al. 2020; Kemp et al. 2020; Kuroyanagi et al., 2020; Hennekam et al. 2020).

The Phanerozoic history of the Earth is marked by periodic OAE (Figs. 1 and 2; Large et al. 2015; Sahoo et al. 2016), followed by an outbreak in planktonic bio-productivity and extinction of more advanced animal and plant groups (Barash 2012; Wang et al. 2015). Such activity resulted in the accumulation of sediments rich in sulfur and organic matter (Khain and Polyakova 2010). There are many known and suspected Phanerozoic oceanic anoxic events which are tied geologically to large-scale production of oil reserves in worldwide bands of black shale in the geological record (Trabucho-Alexandre et al. 2012).

The Paleozoic era oceanic anoxic events

Researchers have documented that oceans were more oxic during early Paleozoic times (Canfield et al., 2008; Poulton and Canfield 2011; Jin et al. 2014; Sperling et al. 2015; Wang et al., 2019a). Nevertheless, many researchers identified ocean anoxia during this time on the basis of geochemical evidences (Poulton and Canfield 2011; Canfield et al., 2008and references therein). The time boundary between the Ordovician and Silurian Periods (i.e., ~443.4 Ma) is marked by repetitive intervals of anoxia, interspersed with normal oxic conditions whereas anoxic conditions were prevalent during the Silurian time (Bartlett et al. 2018). The Ordovician and Silurian boundary time anoxic intervals occurred at a time of low global temperatures (although CO_2 levels were high), in the midst of glaciations. This anoxia is believed to have made major perturbation in ocean chemistry. The Early Paleozoic, marking the oldest recognized Paleozoic OAE, is coeval with the Cambrian explosion of life.

The Mesozoic era oceanic anoxic events

In the Mesozoic, the entire ocean basin transiently became dysoxic or anoxic. During the Cretaceous, ocean anoxic events were characterized by laminated organic-rich shale and low oxygen due to the preservation of trace fossils in the sedimentary record. Various researchers have proposed many OAEs and a number of responsible factors, which occurred alone or in combination during the Mesozoic Era. Silter (1989) demonstrated that during OAEs in this Era, oxygen minimum zones prevailed immediately below the euphotic zone (Wyrtki 1962), which occurred due to oxidation of settling organic material. Beyond the oxygen minimum zone, the preservation of organic material may have been favored by settling rates that are too rapid for the complete oxidation of organic material, and that can be caused by incorporation of organic material in fecal pellets or by aggregation with mineral particles (Tourtelot 1979; Hedges and Keil 1995; Kennedy et al. 2002; Turner 2002).

The three major Oceanic Anoxic Events identified from the Mesozoic record are namely, the Early Toarcian, the Early Aptian, and the Cenomanian-Turonian boundary OAEs. These records are global and are in general characterized by abnormally high organic carbon-rich sediments and locally radiolarian silica. These OAEs are the subject of considerable scrutiny due to the extensive presence of organic carbon in their sediments and all are stratigraphically associated with positive or negative carbon isotope excursions (Scholle and Arthur 1980; Pratt and Threlkeld 1984; Schlanger et al. 1987; Gale et al. 1993). The Early T-OAE occurred under rapid global warming conditions (Baily et al. 2003; Jenkyns 2003) accompanied by mass extinction events (Wignall et al. 2006) and enhanced organic carbon burial (Jenkyns 1988). The Early Aptian is also known as Livello Selli in the type section of Italy are characterized by a pronounced negative carbon isotope excursion followed by a positive excursion in deep and shallow marine carbonate, marine matter, and terrestrial higher plants (Gröcke et al., 1999; Jenkyns, 1999, 2003; Herrle et al., 2004; Van Breugel et al. 2007). This pronounced negative carbon isotope excursion is perhaps the most distinctive feature of OAE 1a on a global scale and it coincides with the lowest stratigraphic level of the organic-rich shales themselves (Jenkyns 2010). Jones and Jenkyns (2001) discussed in detail the causes behind three well-documented OAEs in the Mesozoic Era which occurred in the early Jurassic, the early and late Cretaceous times.

Since the beginning, the OAEs have been commonly and globally identified from the Mesozoic time span of Earth's geological history and Fig. 2 shows the compilation of major OAEs during Mesozoic as illustrated by Jenkyns (2010). According to Jenkyns (2010), major Mesozoic OAEs include early Toarcian (Posidonienschiefer event, T-OAE, ~183 Ma), early Aptian (Selli event, OAE 1a, ~120 Ma), early Albian (Paquier event, OAE 1b, ~111 Ma), and Cenomanian-Turonian (Bonarelli event, C/TOAE; OAE 2, ~93 Ma) OAEs. Jenkyns, 2010, Fig. 2) also documented some other OAEs in the Cretaceous, particularly those from Tethyan region: OAE1c (the record is patchy; Arthur et al. 1990; Tiraboschi et al. 2009), OAE 1d (late Albian Breistroffer event; Arthur et al. 1990), early Cretaceous Valanginian Weissert event (Lini et al. 1992; Erba et al., 2004; Brassell 2009 and references therein), latest Hauterivian Faraoni event (Baudin 2005; Bodin et al. 2007). Likewise, the late Coniacian to Santonian age OAE is represented as OAE 3 (Arthur et al. 1990; Wagner et al. 2004).

There had been considerable research focus on Mesozoic OAEs since several decades. The regions of sub-Mediterranean, sub-Borealand Boreal provinces of Europe have been extensively explored (Stoll and Schrag 2000; Hesselbo et al. 2007 and references therein; Tsiko et al. 2004; Lehmann et al., 2012; Najarro et al. 2011; Bottini and Mutterlose 2012; Millán et al., 2014; Boulila and Hinnov 2017; Percival et al. 2020 and many more). Amongst other Mesozoic OAE records have been documented from Argentina (Al-Suwaidi et al. 2010; Richiano 2014 and references therein), southeastern China (Hu et al. 2014; Joo et al. 2020 and references therein), northern margin of Africa (Soua 2014; Godet et al. 2014), Asia (Li et al. 2006; Takashima et al. 2010), North America (Sageman et al. 2006; Elrick et al. 2009), and South America (Navarro-Ramirez et al. 2016). The three major oceanic anoxic events identified from the Mesozoic record namely early Toarcian, early Aptian, and Cenomanian–Turonian OAE have records of global distribution and are stratigraphically associated with positive carbon-isotope excursions as well as paleo-temperature maxima.

Triassic Period Widespread oceanic anoxia conditions at the beginning of the Triassic period have been reported on the basis of geochemical evidence, cerium anomalies, and carbon/sulfur ratios (Hallam 1994). This is also supported by the occurrence of extensive anaerobic and dysaerobic facies as well as the absence of reef and associated high diversity benthic communities. These have been further tested by sedimentary facies and sequence stratigraphic analysis of key sections across the Permian-Triassic boundary in the former Paleo-Tethys region in Italy, Pakistan, and China (Wingnall and Hallam 1992; Knoll et al. 1996; Krull and Retallack 2000; Becker et al. 2001; DeWit et al. 2002; among others). Various results suggest that the youngest Permian faunas became extinct at the beginning of the Triassic period, as a consequence of the extensive spread of anoxic waters into epicontinental seas associated with then marine transgression.

Jurassic Period In the Jurassic period, one major OAE i.e. Toarcian oceanic anoxic event (~183 Ma) has been documented (Harries and Little 1999; Bailey et al. 2003; Cohen et al. 2004). The reason being no deep-sea drilling projects were undertaken because of the little or no Toarcian crust remaining in the world's oceans (Harries and Little 1999; Jenkyns 1988). The remains of Jurassic organic matter are found in many places like NE and central Tunisia (Soussi, 2003; El Asmi et al. 2003; Fauré and Peybernès, 1986; Bonnerfous 1972). This global anoxic event had been first observed in Tunisia (Soussi et al. 1990), however, no significant work on such accumulations had been done since long. And this event in the Jurassic became a source of attention only in the last few years due to hydrocarbon exploration in the middle and high latitudes of the northern hemisphere, such as Western Europe and Russia (Soua 2014). The boundary of Ordovician and Silurian is indeed marked by repetitive anoxia; however, detailed OAE studies are still lacking in the Tethyan realm.

Cretaceous Period Jenkyns (2010) compiled data and documented the presence of at least seven oceanic anoxic events during the Cretaceous period (Fig. 2). It is widely demonstrated that this period had a warm climate accompanied by greenhouse gases (Huber et al. 2002; Littler et al. 2011; Friedrich et al. 2012). This warm climate is quantitatively evidenced by the presence of thermocline floras and faunas at higher latitudes during the Cretaceous time (Nathorst 1890; Frakes et al. 1992; Frakes 1992; Tarduno et al. 1998; Fig. 1). The eustatic sea level during the Cretaceous was on average 75–250 m higher than present-day mean sea level (Miller et al. 2005; Macleod et al. 2013), though some evidence of small-scale glaciation during the early and late Cretaceous have been reported (Bornemann et al. 2008). The proper understanding of the spatial, absolute, and temporal variation of temperature during Cretaceous time is vital to elucidate the exact nature of greenhouse gas forcing, climate sensitivity, and ocean circulation at that time (Friedrich et al. 2012; Royer et al. 2012; Wang et al. 2014).

The Cenomanian-Turonian is the most widespread and best-defined OAEs of mid-Cretaceous. Arthur and Schlanger (1979) and Jenkyns (1980) have shown major fluctuations in carbon isotope near the Cenomanian-Turonian boundary. They related this fluctuation to changes in ocean circulations in the Atlantic Ocean, wherein an expanded oxygen minimum layer formed. During this time organic-rich sediments were deposited in a variety of paleobathymetric settings like ocean plateau and basin, continental margin, and shelf. The widespread depositional nature of these sediments indicates that they were not controlled by local basin geometry but were a product of global to regional oceanic anoxic conditions. This is further supported by the reports of marine transgression during the Cretaceous time, wherein both area and volume of shallow epicontinental and marginal seas were accompanied by an increase in the production of organic carbon.

According to Jenkyns (2010), major OAEs include early Aptian (Selli event, OAE 1a, ~120 Ma), early Albian (Paquier event, OAE 1b, ~111 Ma), and Cenomanian-Turonian (Bonarelli event, C/TOAE 2, OAE ~93 Ma). Jenkyns (2010; Fig. 2) also documented some other OAEs in the Cretaceous, particularly those from the Tethyan region: OAE1c (the record is patchy; Arthur et al. 1990; Tiraboschi et al. 2009), OAE 1d (late Albian Breistroffer event; Arthur et al. 1990), early Cretaceous Valanginian Weissert event (Lini et al. 1992; Erba et al., 2004; Brassell 2009 and references therein), latest Hauterivian Faraoni event (Baudin 2005; Bodin et al. 2007). Likewise, the late Coniacian to Santonian age OAE is represented as OAE 3 (Arthur et al. 1990; Wagner et al. 2004).

The Cenozoic era oceanic anoxic events

The Paleocene-Eocene epoch of the Cenozoic remarkably share features similar to those of Palaeozoic and Mesozoic oceanic anoxic events. The PETM in the Cenozoic is the only identified OAE in this Era (Kennett and Stott 1991; Jenkyns 2010 and references therein). Many researchers believe PETM to be the last OAE of the Phanerozoic; even those who do not consider it to be the last one, still believe it as one of the OAE due to many related common characteristics with other well established OAEs (Scharag and Higgins 2006; Jenkyns 2010). For example, Kennett and Stott (1991) first identified PETM as OAE on the basis of an abrupt increase in global temperatures. Later a number of similarities with other OAEs, particularly with the early Toarcian OAE, have been demonstrated. In a manner similar to T-OAE, this OAE showed increased organic productivity concentration on the shelf regions rather than deep sea as well as a positive shift in sulfur isotope ratios and shift of osmium values toward more radiogenic values indicating increased continental weathering, increased carbonate compensation depth and also evidence of coeval North Atlantic Large Igneous Province event (Speijer and Wagner 2002; Cohen et al. 2004, 2007; Sluijs et al. 2008; Zeebe et al. 2009; Jenkyns 2010; Bottini et al., 2012; Du Vivier et al., 2014; Jenkyns et al. 2017). According to Jenkyns (2010), the PETM did not develop into full- blown OAE because climatic forces were probably not of sufficient intensity to fertilize extensive area of the ocean and paleogeography was not conducive for water column stratification except in the Arctic Ocean.

Research related to OAEs in India

Significant research has been carried out on OAEs in different parts of the world. However, they are not as widely investigated in India when compared to the other parts of the world. Table 2 shows a compilation of possible OAEs in major geological formations of India which are correlatable with globally reported OAEs. In India, early Aptian 1a in the Giumal Formation of early Cretaceous and probably an early Albian OAE 1b, late Albian OAE 1c, and 1d, latest Cenomanian/Santonian OAEs in the Chikkim Formation have been documented Bertle and Suttner 2005; Bhargava 2008; Pathak et al. 2011). Similar to OAE 1a, another location is a Ukra member in the Umia formation of Kutch (Pandey and Pathak 2016). The globally important and equivalent anoxic events like OAE-1b, OAE 1d, OAE-2, and OAE-3 have been identified in the Narmada and Cauvery basins of India (Cronin et al. 2010; Nagendra and Reddy 2017; Bansal et al. 2019; Keller et al., 2021).

The Cretaceous anoxic events in the Indian part of geology are represented by black shales having pyritic nodules and fossil wood found in the late Cretaceous Mahadeo formation (Lokhu and Tiwari 2011). Krishna (1983) documented ammonoid-rich, green shales of Umia formation (Kutch) of the early Aptian age as a suitable site of OAE. The green color of shale is probably because of its deposition in the extreme marginal location of the Kutch basin. The Jhuran Formation of Kutch is considered equivalent to Selli oceanic anoxic event (Krishna 1983). The ammonoid-rich Spiti and Guimal formations (Bhargava 2008) are also suitable OAE representatives. The Spiti formation unit is about 210 m thick and is part of a folded sequence of argillaceous lithology comprising black splintery shale and limestone (Krishna et al. 1983). Black to gray-green sediments in Jurassic-Cretaceous of Spiti valley can be correlated with globally well-known oceanic anoxic events. Black shales of the early Himalayan foreland basin sediments which coincide with the India-Eurasia collision and PETM may represent the last global OAE (Jenkyns 2010). Sundaram et al. (2001) demonstrated that the Albian to Maastrichtian age (i.e., early to late Cretaceous) marine sediments in the Cauvery basin which have ammonoid bearing horizons and black shales indicate some similarity to global OAEs ranging from OAE 1a to OAE 3 (as compiled by Jenkyns 2010).

Arora et al. (2015) demonstrated the possibility of OAE in the Mesozoic geologic history of the Kutch basin (India) in a manner similar to the globally established OAEs during that time. They carried out detailed sedimentary facies and organic geochemical studies of the Jurassic Jhuran Formation of Kutch. The Jhuran Formation has organic-rich, dominantly black shales which are alternating with thin to thickly bedded siltstone with minor sandstones. In the studied middle Member of the Formation, they identified five

Table 2 Globally identified OAEs and their equivalents in India

Era	Period	Epoch	World	India
Mesozoic (250–65 Ma)	Jurassic		Toarcian event (183 Ma)	Juran Formation of Kutch[1]
			Posivonienschiefer event (182.7 Ma)	Kioto Formation (Tangling Group) of Spiti[2]
	Cretaceous	Lower	Aptian: mid-Aptian extinction event 116 ± 7Ma	Cretaceous organic rich shale of Cauvery basin (OAE-1b, OAE-1d, OAE-2, OAE-3)[3]
			Paquier event (112 Ma)	Terani Formation OAE-1b in the Cauvery basin[4]
			Breistroffer event (99.6 Ma)	Late Albian–Cenomanian OAE-1d in western margin of Cauvery basin[5]
	Cretaceous	Upper	Cenomanian–Turonian boundary event: black shale deposition in ocean 91.5 ± 8.6 Ma	Chikkim Formation in the Spiti area[2]
			Bonarelli event (93.6 Ma)	Late Cenomanian to Early Turonian OAE-2 in the Cauvery basin[5]
				Late Cenomanian to Early Turonian in western part of Narmada basin (M.P.)[6]
				Coniacian–Santonian OAE-3 in the Cauvery basin[5]
Cenozoic (65 Ma)	Tertiary	Paleocene Eocene	Thermal maximum ~55.8 Ma	Cambay basin[7]
				Early Himalayan Foreland Basin sediments

[1]Arora et al. (2015); [2]Pandey and Pathak (2016); [3]Nagendra and Reddy (2017); [4]Nallapa et al. (2013); [5]Cronin et al. (2010); [6]Keller et al. (2021); [7]Samanta et al. (2012)

litho-facies namely, facies A: Black shale, facies B: Black shale inter-bedded with siltstone, facies C: alternations of shale and siltstone with minor sandstones, facies D: alternations of siltstone-sandstone, and facies E: plane laminated and hummocky cross-stratified sandstone. Besides litho-facies analysis, geochemical investigations that have been carried out include TOC, OI, HI, T_{max}, and trace element analysis. It has been documented by them on the basis of their analyses that the black shales of facies A and B could be possible indicators of oceanic minimum zones (OMZ) which had been extended to shallow seas due to a rise in global sea level during the formation of OAE. Also, calculated average values of Ni/Co and V/(V + Ni) ratios are, respectively, 2.5 and 0.82, and 7–20-μ size of pyrite framboids, indicating the prevalence of intermittent anoxic and sulfidic conditions during the deposition of these sediments. Finally, Arora et al. (2015) concluded that the black shales of the Jhuran Formation possibly carry signatures of late Jurassic OAE and further require detailed studies.

In the Indian part, other most important globally defined anoxic events viz. OAE-1b, OAE-1d, OAE-2, and OAE-3 are fairly identifiable in the Cauvery basin of the southern part of India (Cronin et al. 2010; Nagendra and Reddy 2017). Nagendra and Reddy (2017) demonstrated major transgressive episodes in the Aptian-Paleocene sediments exposed in the Ariyalur district of the Cauvery basin. This led to oxygen-depleted conditions during late Aptian-early Albian (OAE 1b), late Albian (OAE 1d), and late Cenomanian-early Turonian (OAE 2) times, therein resulting in deposition of organic-rich sediments. Nagendra and Reddy (2017) further suggested the prevalence of anoxic conditions during Coniacian-Santonian (OAE 3) and Campanian age sediments in this region on the basis of some evidence. These all correlate well with the local peaks of transgressive cycles (Nagendra and Reddy 2017 and references therein). Very recently, Keller et al. (2021) worked in the Narmada basin in India and studied in detail OAE 2 on the basis of detailed investigations in two outcrops from Bagh Formation sediments in the Gujarat state of India. Their major investigations focused on biostratigraphy, δ^{18}O records, and carbon isotopes for identification of the Cenomanian-Turonian OAE as well as the potential influence of LIP on the basis of mercury concentration in the sediments. Keller et al. (2021) on the basis of their results revealed that in the western Narmada basin, the onset of OAE2 δ^{13}C excursion during late Cenomanian coeval with the sea-level transgression and the age of transgression is well correlatable with the Pueblo, Colorado, Global Section, and Stratotype Point (GSSP), and the eastern Sinai Wadi El Ghaib section of Egypt.

Major factors documented for formation of OAEs

LIPs/volcanic eruptions

The Earth's geological history witnessed the emplacement of enormous igneous material into the continental and oceanic crust and these are known as LIPs. It is well established that these igneous emplacements and/or volcanic eruptions cause significant severe to catastrophic effects on climate and environment (Wignall 2005 and references therein, Percival et al. 2015). For example, Wignall (2005) illustrated through a flow chart (Supplementary Fig. 1) that how the LIP eruptions bring changes in major biogeochemical processes related to Earth's environment and climate. Rapid global warming, oceanic anoxia, or increased oceanic fertilization or both, calcification crises, mass extinctions, a sharp decrease in δ^{13}C values recorded in limestones, are some of the major environmental and climate effects due to LIP eruptions as compiled by Wignall (2005). A number of researchers have documented temporal correlation of LIPs with OAEs (Fig. 1) and this correlation is best demonstrated for these events in the Mesozoic Era. Percival et al. (2015) compiled a temporal correlation of various volcanic/LIP events and OAEs as well as mass extinction events during the Phanerozoic Eon (Fig. 1). They demonstrated that such correlation was limited during the Palaeozoic Era because Palaeozoic provinces are less likely to be preserved whereas radiometric ages of various Mesozoic LIPs coincide with dates of OAEs during Mesozoic Era. The temporal correlation between LIPs and OAEs are again limited during Cenozoic Era because Cenozoic provinces were emplaced in an icehouse climate, wherein it is less likely to accelerate regional anoxic conditions (Percival et al. 2015).

Large scale volcanism is reliably considered to be one of the reasons behind the oceanic anoxic events due to the enormous release of a large quantity of carbon dioxide into the atmosphere as well as through dissociation of methane hydrates and thermogenic methane leading to rapid global warming (Robinson et al. 2017; Valle et al. 2019). Researchers have widely considered a direct link between LIPs and OAEs throughout the Phanerozoic Eon. This is perhaps due to the fact that in the geological history of Earth, the regional to global scale OAEs occurred during the rapid, persistent greenhouse (i.e., global warming) state of the Earth (Fig. 1). For example, the Mesozoic Era represents the greenhouse state and substantial evidence of rapid global warming during the Jurassic and Cretaceous periods have been reported. Various studies have arrived at a consensus that the LIPs played a significant role in triggering OAEs during the Jurassic and Cretaceous periods resulting in mass extinctions (Fig. 1 and Supplementary Figs. 2 and 3). Among the various OAEs, the T-OAE; Posidonienschiefer event) during Early Toarcian of the Jurassic Period (~183 million years ago), the Early Aptian Oceanic Anoxic Event (OAE 1a, Selli Event) during Aptian of the Cretaceous Period (~120 million years ago), and the Cenomanian-Turonian Oceanic Anoxic Event (C/TOAE; OAE 2; Bonarelli Event) at the boundary of Cenomanian-Turonian of the Cretaceous Period (~93 million years ago) occurred on a global scale and have been commonly studied by researchers in a number of outcrops at different parts of the world. These major global scale OAEs have been directly linked by researchers with coeval LIPs.

For example, Percival et al. (2015) worked on the direct link between Karoo-Ferrar LIP and the coeval T-OAE on the basis of detailed studies on mercury (Hg) concentrations and their behavior in atmosphere and sediments under various conditions at different spatial scales. Percival et al. (2015) showed the potential of Hg element and Hg/TOC ratios as a global scale proxy for LIP volcanism and further documented the relationship between Karoo-Ferrar LIP and the T-OAE. Later, Boulila and Hinnov (2017) also demonstrated on the basis of carbon isotope excursion (CIE) that there was a massive injection of ^{12}C into the ocean and atmosphere/hydrosphere reservoirs from volcanic greenhouse gases and linked the global warming to Karoo-Ferrar LIP which finally brought changes in climate leading to vast oceanic anoxia and the formation of T-OAE. Likewise, the global scale Cenomanian-Turonian Oceanic Anoxic Event (C/T OAE; OAE 2; Bonarelli Event) at the boundary of Cenomanian-Turonian of the Cretaceous Period (~93 million years ago) occurred when there is substantial evidence of the occurrences of several large-scale igneous provinces in Madagascar, the Caribbean-Colombian, Ontong Java II. Very recently, Joo et al. (2020) made a detailed compilation of various environmental changes which led to this oceanic anoxic event (i.e., OAE 2) and they also assessed the enormous studies which documented that the Caribbean LIP played a major role in triggering OAE 2.

Eustatic sea level change

The eustatic/global sea-level change represents the changes in sea level of the total volume of Earth's oceans. Major changes in eustatic sea-level bring changes in sedimentary deposits of marine environments, as such changes strongly control accommodation space leading to marine transgression and regression phases. Thus, sea-level change is an important parameter in controlling the expansion of oxygen-depleted conditions in neritic settings during OAEs and major changes in sea level are commonly associated with OAEs (e.g., Supplementary Fig. 4). Despite its fundamental role, on a short scale (<1 Ma) it remains one of the least constrained parameters for numerous OAEs. It has been documented that phases of marine transgression and regression occur during formation of the OAEs. For example, the sedimentological and geochemical evidence from Morocco and East Greenland showed that a forced regression shortly precedes (ca.10^2 kyear) the major transgression associated with Toarcian OAE (Krencker et al., 2019). The sea-level fluctuation has important implications for the organic products of the ocean and sediment distribution pattern along the continental margin and in the interior basin. Due to these fluctuations, this also becomes important for hydrocarbon exploration.

The sea-level changes control hydrographic-climatic patterns as well as biotic distribution. Knowledge of these sea-level changes led to a better understanding of global changes in environment and climate (Ganguly et al. 2015) and, therefore, OAEs, particularly those of the Mesozoic and Cenozoic Era. For example, major environmental perturbations occurred during the early T-OAE of the Mesozoic Era. This T-OAE was associated with important faunal and floral turnover as well as soaring global temperatures and increased tropical cyclone intensity. The T-OAE is best characterized by a high amplitude negative carbon isotope excursion as recorded from carbonate micrite, bulk organic matter, wood debris, brachiopod valves, biomarkers, and organic matrix of belemnite rostra (Rita et al. 2020). This has been observed in both shallow- and deep-water settings widely distributed over several terranes underlining the global character of this carbon cycle perturbation. Generally, a causal link between the emplacement of the Karoo-Ferrar large igneous province and the initiation of the T-OAE is postulated due to the synchronicity of these two events. However, the exact mechanism responsible for the faunal and floral turnover at the onset of the T-OAE remained uncertain besides the exact causes of the negative CIE until the end of the nineteenth century when various researchers explained these on evidence of gas hydrate dissociation as discussed in succeeding section.

Nevertheless, researchers have well established that the creation/destruction of shallow-marine habitats due to changes in sea level is known to be a primary control of marine biotic diversity. Despite this, and the equally important role of relative sea-level change in guiding oceanographic currents and the development of anoxic bottom water, there is currently no consensus about the amplitude and interpretation of early Toarcian high-frequency sea-level changes (Hermoso et al. 2013). It is commonly accepted that, following the latest Pliensbachian "Spinatum" lowstand, the early Toarcian corresponds to a long-term transgression associated with a global sea-level rise, initially invoked as a cause for basinal anoxia/euxinia during the T-OAE (Krencker et al., 2019). However, several studies have highlighted that a short-term regressive event characterizes the upper part of the Polymorphum Zone (Pittet et al. 2014). Nevertheless, it remains elusive if this was only a normal regression (i.e., progradation driven by sediment supply outpacing the rate of base-level rise at the coastline) or if it was coupled to a forced regression (i.e., progradation driven by base-level fall). Presently, the amplitude of the sea-level rise that contributed to the overall Toarcian transgression is unconstrained as well as its exact cause and role in the unfolding of the T-OAE (Krencker et al., 2019)

In general, researchers have widely shown that the global OAEs in Earth's history are largely restricted in specific sedimentary facies, i.e., gray to black shale facies, which are commonly organic-rich. The concentration of organic matter in distinct, widely distributed beds of black shale has been facilitated by reduced terrigenous sedimentation during transgression and/or the incursion of upwelling induced oxygen minima across the upper slope and shelf with rising sea level (Hallam and Bradshaw 1979; Arthur et al. 1987; Schlanger et al. 1987; Arthur et al. 1990; Arthur and Sageman 1994). Indeed, Arthur and Sageman (1994) discussed in detail black shales and their depositional regimes in the stratigraphic record, particularly the Cretaceous age organic-carbon rich black shales confined during then OAEs. They documented that the most widespread such organic-rich, shale depositional events correspond with overall higher sea level stands (at global/regional scale). Very recently, Keller et al. (2021) explored the link between first sea-level transgression in the western Narmada basin (Gujarat, India) during late Cenomanian to early Turonian OAE2. They demonstrated that the sea-level transgression and the OAE 2 $\delta^{13}C$ excursion during the late Cenomanian to early Turonian in the Narmada basin (India) well correlated with the Pueblo, Colorado, GSSP, and the eastern Sinai Wadi El Ghaib section of Egypt.

Dissociation of gas hydrates

Researchers have also documented association of OAEs with climate warming caused due to dissociation of gas hydrates (Hesselbo et al. 2000 and references therein; Heydari and Hassanzadeh 2003; Song and Woodcock, 2003; Röhl et al., 2007; Hesselbo and Pieńkowski, 2011; Ruebsam et al. 2019 and references therein). Methane gas hydrates have also been found in the sub-surface sediments in permafrost regions, besides their common occurrence in marine/oceanic sediments, particularly on the sea floor on continental margins. What needs attention is that these marine gas hydrates are very sensitive to the temperature and pressure stability fields and therefore even slight changes in temperature and/ or pressure conditions on the sea floor can result in rapid dissociation of gas hydrates in to hydrocarbon gases, largely methane.

The release of enormous methane into the natural environment, to the ocean, and atmosphere strongly affects the balance between hydrosphere-lithosphere-atmosphere resulting in major changes in the global carbon cycle and climate (Hesselbo et al. 2000; Song 2003 and many more). Kennett et al. (1991) demonstrated that the gas hydrate dissociation significantly increases global temperature resulting in increased global warming and catastrophic chain reactions are further triggered. It has been well-established that methane is an important greenhouse gas, about 20 times larger than the same volume of carbon dioxide. Extensive dissociation of gas hydrates resulting in increased release of methane would subsequently create anoxic conditions in the sea-water and ultimately in the atmosphere which may cause mass extinction. Thus, gas hydrate dissociation data/ records would be significant in understanding the various global warming events in the Earth's history as well as the present and future changes in climate.

Substantial studies in the last two decades from geologic records have revealed that gas hydrate dissociation played an important role in controlling sea-level fluctuations, climate warming events, and occurrence of OAEs in the Earth's geological history before the Quaternary period. For example, Bratton (1999) documented a mechanism of methane gas hydrates controlling sea level on the basis of clathrate eustasy whereby anomalous sea level falls during greenhouse periods of the Devonian, the Cretaceous, and the early Eocene. In other words, expected sea-level rise due to thermal expansion can be offset by a decrease of gas hydrate volume due to their dissociation. Likewise, Heydari et al. (2003) discussed in detail the Permian-Triassic boundary (PTB) anoxic event on the basis of the accumulation-dissociation cycle (Heaven-Hell cycle) of methane gas hydrates. Heydari et al. (2003) further elucidated the periodicity of OAEs and mass-extinctions on the basis of methane hydrates accumulation-dissociation cycles during the Phanerozoic Eon.

The Earth's geologic history witnessed several greenhouse/ hyperthermal periods, wherein negative carbon isotope excursions (CIEs) have been well explained on the evidence of periodic gas hydrate dissociation events (e.g., in the Early Cretaceous by Jahren et al. 2001; in the Early Jurassic sediments by Hesselbo et al. 2000; in the Late Jurassic sediments by Padden et al. 2001; in the Paleocene-Eocene by Matsumoto 1995 and Dickens et al. 1995). The early T-OAE in the Jurassic period has been documented to have shown important global perturbations in carbon-cycle and climate. It is characterized by exceptionally high rates of organic carbon burial, high palaeotemperatures, and significant mass extinction (Hesselbo et al. 2000). In a manner similar to some other hyperthermal periods, the origin of such distinct, 3–8‰ negative CIE during this early T-OAE has been commonly debated with no acceptable view. However, the possibility of gas hydrate dissociation in marine-continental margin sediments resulting in rapid release of excessive methane could readily explain such a pattern of large, negative CIEs (Hesselbo et al. 2000; Jiang et al. 2003). Likewise, such trend in CIEs from the study of marine and terrestrial sediments during one of the most widely studied hyperthermal periods, PETM at ~54.95 Ma, has been explained on the basis of methane hydrate dissociation (Matsumoto 1995; Dickens et al. 1995; Dickens 2001, Zachos et al. 2005; Röhl et al., 2007).

Impact events: asteroid impacts

Major impact events have been reported in the Earth's history and are commonly considered to be responsible for various mass extinctions. Rumpf et al. (2017) defined an impact event as a collision between astronomical objects (e.g., asteroids, meteorites, or comets on planets) resulting in considerable effects on all-natural spheres. On terrestrial planets, like our Earth, effects due to impact events depend on a number of factors, and depending on astronomical body size would result in regional to global scale earthquakes, tsunamis, and other natural hazards. If an asteroid hits on Earth's land surface then it would result in enormous dust in the atmosphere whereas if it hits Earth's water bodies then it would result in significant water vapor in the atmosphere. Subsequently, this would result in dust-storms, fire-storms, rain-storms bringing severe changes in the atmosphere and consequently effects on the biosphere. There are more than hundreds of reported impact events in the Earth's recorded history, whereby catastrophic effects have been documented. Similarly, researchers have geological evidence of past impact events in the Earth's Pre-Quaternary history (Alvarez et al. 1980; Smit and Hertogen 1980; Wolbach et al. 1988 and references therein; Hildebrand et al. 1991; Kaiho and Lamolda 1999; Norris et al. 1999; Pierazzo et al. 2003; Schulte et al. 2010; Ohno et al. 2014; Kaiho et al. 2016; Kaiho and Oshima 2017; Witts et al. 2018; Chiarenza et al. 2020 and references therein). These impacts significantly changed climate, including the formation of OAEs, and subsequently resulted in mass extinctions.

The Permian-Triassic mass extinction (about 250 Ma ago) is one of the greatest mass extinctions on Earth. Substantial studies have been done to understand the cause behind this mass extinction, however, reached no consensus. Muller et al. (2005) associated this mass extinction with impact event on the evidence of age and origin of an impact crater namely "bedout high structure." In general, impact craters and structures are the most common landforms created by various impact events. Similarly, the Cretaceous-Paleogene (K-Pg boundary) mass extinction at about 66 million years ago is most commonly associated with asteroid impact events (Chiarenza et al. 2020 and references therein). As soon as the beginning of nineteen eighties, Alvarez and his team of researchers (Alvarez et al. 1980) noticed unusually high concentrations of iridium element in ~65-million-year-old rock strata whose distribution was found worldwide, thereby indicating them to conclude the possibility of the collision of a large asteroid. However, such unusual iridium enrichment can also be caused by volcanic events. The volcanic origin was discarded by Shukolyukov and Lugmair (1998) on the basis of anomalies in chromium isotopic ratios which were indeed very similar to those observed in carbonaceous asteroids. Carter et al. (2010) supported this asteroid impact on the basis of the presence of coesite mineral which is typical of large impact events. However, the discovery of the "Chicxulub" crater on the Yukatan Peninsula of Mexico forms the most robust evidence for this asteroid impact occurrence at the Cretaceous-Paleogene boundary (Pierazzo et al. 2003; Schulte et al. 2010).

Taking the example of the Chicxulub-scale asteroid, Kaiho et al. (2016) and Kaiho and Oshima (2017) demonstrated that massive soot presence could be the main cause of mass extinction after an asteroid impact. Kaiho et al. (2016) did detailed documentation of direct evidence for stratospheric soot at the K-Pg boundary due to Chicxulub asteroid impact. They demonstrated the global level spread of massive amounts of soot which efficiently absorbed and scattered sunlight in the stratosphere. This affected the global climate because the soot aerosols brought severe cooling and subsequently cessation faunal food productivity on land and in global oceans resulting in mass extinction. Later on, Kaiho and Oshima (2017) clearly showed how and why the amounts of stratospheric soot and sulfate sourced from asteroid impact would vary at various global locations. Recently (Chiarenza et al. 2020) compiled various data to compare asteroid impact and Deccan volcanism drivers for the K-Pg mass extinction and global climate change. They illustrated that the Chicxulub asteroid impact severely affected climate and global ecosystems and concluded this impact as the major driver of mass extinction because even the highest assumed intensity of sulfates due to Deccan volcanism, barely approaches the lowest estimates of release by Chicxulub impact.

Tectonic changes

Researchers have documented that one of the factors responsible for the formation of oceanic anoxic conditions is the changes in tectonic conditions, particularly greater rates of seafloor spreading, submarine volcanism, and hydrothermal activity coupled with rising sea level and global warming (Leckie et al. 2002 and references therein). For example, the mid-Cretaceous time period (~124–90 Ma) records a number of major OAEs and this is also the time wherein increased tectonic rates, changes in paleogeography have been documented which resulted in changes in the ocean-climate system (Larson and Pitman 1972; Hays and Pitman 1973; Arthur et al. 1985; Kominz 1984; Barron 1987; Larson, 1991; Richter et al. 1992; Jones et al. 1994; Ingram et al. 1994; Hay 1995; Clarke and Jenkyns 1999; Poulsen et al., 1999, 2001; Jones and Jenkyns 2001; Leckie et al. 2002). Reports of increased rates of seafloor spreading and ridge length during Aptian which subsequently with time resulted in a eustatic rise in sea level during Albian-Turonian have been found. For example, Richter et al. (1992) gave 40–50% higher rates of seafloor spreading during the mid-Cretaceous than what they are in the present time.

Leckie et al. (2002) discussed in detail the tectonic forcing during mid-Cretaceous and to what extent tectonically driven changes controlled spatial and temporal distribution of the OAEs. They demonstrated that the OAEs of the latest Albian and Cenomanian/Turonian boundary had been caused by different tectonic and ocean-climate conditions than the early Aptian and latest Aptian–early Albian events. Thus, accelerated ocean crust production along with active mid plate and plate margin volcanism subsequently triggered greenhouse conditions and consequently rising sea level which finally resulted in oceanic anoxic to dysoxic conditions.

Ocean stratification

Ocean stratification/layering occurs when water masses of different densities meet, wherein lower density water is on top of higher density water. In particular temperature and salinity are the major properties controlling density and the greater the differences in the properties between layers, the less mixing occurs between the layers. Stratification is increased when the temperature of the surface ocean or the amount of freshwater input into the ocean from rivers and ice-melt increases, thereby intensifying ocean deoxygenation. Ocean deoxygenation results in suboxic, hypoxic, and anoxic conditions in both coastal waters and the open ocean. Several areas of the open ocean are called oxygen minimum zones (OMZs) when they show naturally low oxygen concentration due to biological oxygen consumption which cannot be supported by the rate of oxygen input to the area from physical transport, air-sea mixing, or photosynthesis (Breitburg et al. 2018).

Most ocean anoxic events are thought to be caused by high productivity and the export of carbon from surface waters which are then preserved in organic-rich sediments, known as black shales (Erbacher et al. 2001). The accelerated hydrological cycle during OAEs plays a key role in supplying nutrients to the coastal water and enhancing stratifications contributing to the development of ocean anoxia (Dera and Donnadieu, 2012). The decrease in salinity during OAE 2 due to enhanced runoff resulted in increased stratification along the continental margin which led to water column deoxygenation (van Helmond et al. 2014). The Euxinic conditions have been favored due to restrictions of the ocean/seaway, however, increased freshwater input promoted water column stratification. Such kinds of increased stratification of the water column by surface water warming and/or increased runoff indicate that black shale formed as a mega sapropel as an analogy to Plio-Pleistocene sapropel accumulation in the Mediterranean Sea (Kuypers et al. 2001).

Paleocene-Eocene HFB sediments: possibility of OAE

The end of the Paleocene and the beginning of Eocene geological epochs in the Cenozoic Era is marked by an abrupt rise in temperature and the major changes in Earth's carbon cycle. Earlier this climate event at the boundary of Paleocene-Eocene was known as "Initial Eocene Thermal Maximum" or "Late Paleocene Thermal Maximum" but now popularly known as "PETM," if not "Eocene Thermal Maximum 1 (ETM1)." A wide array of researchers has studied in detail the PETM due to various reasons and majority of the researchers consider it as an analog to understand global warming. It has already been mentioned in the preceding sections that the only identified OAE in the Cenozoic which is also believed to be the last OAE of the Phanerozoic could perhaps form during the PETM. Kennett and Stott (1991) first documented this on the evidence of an abrupt increase in global temperatures. McInerney and Wing (2011) compiled in detail and revealed an increase in global temperatures by 5–8 °C whereas earlier interpreted the increase in global temperatures by ~5 °C. Thus, it was obvious for researchers to believe PETM as a representative OAE because major global OAEs have been recorded during increased global temperatures (i.e., greenhouse conditions) in Earth's history. A number of causes like large-scale volcanism, biomass burning, impact event, permafrost thaw, gas hydrate dissociation, and tectonic changes have been put forth by researchers to explain PETM; however, methane hydrate dissociation remains the most commonly accepted. Jenkyns (2010) observed that the Palaeocene-Eocene Himalayan foreland basin sediments, which coincide with the India-Eurasia collision and PETM share many features and phenomena in common to other OAEs and thus may represent another global OAE.

The Himalayan Foreland Basin (HFB) is the southernmost subdivision of the five litho-tectonic subdivisions of the Himalaya (Dutta et al. 2019). Detailed geology and stratigraphy of the HFB have been compiled by a number of researchers (Raiverman 2002; Acharyya 2007; Jain et al. 2009, etc.). The HFB comprises sediments of shallow marine facies to brackish-fresh water molasse facies and

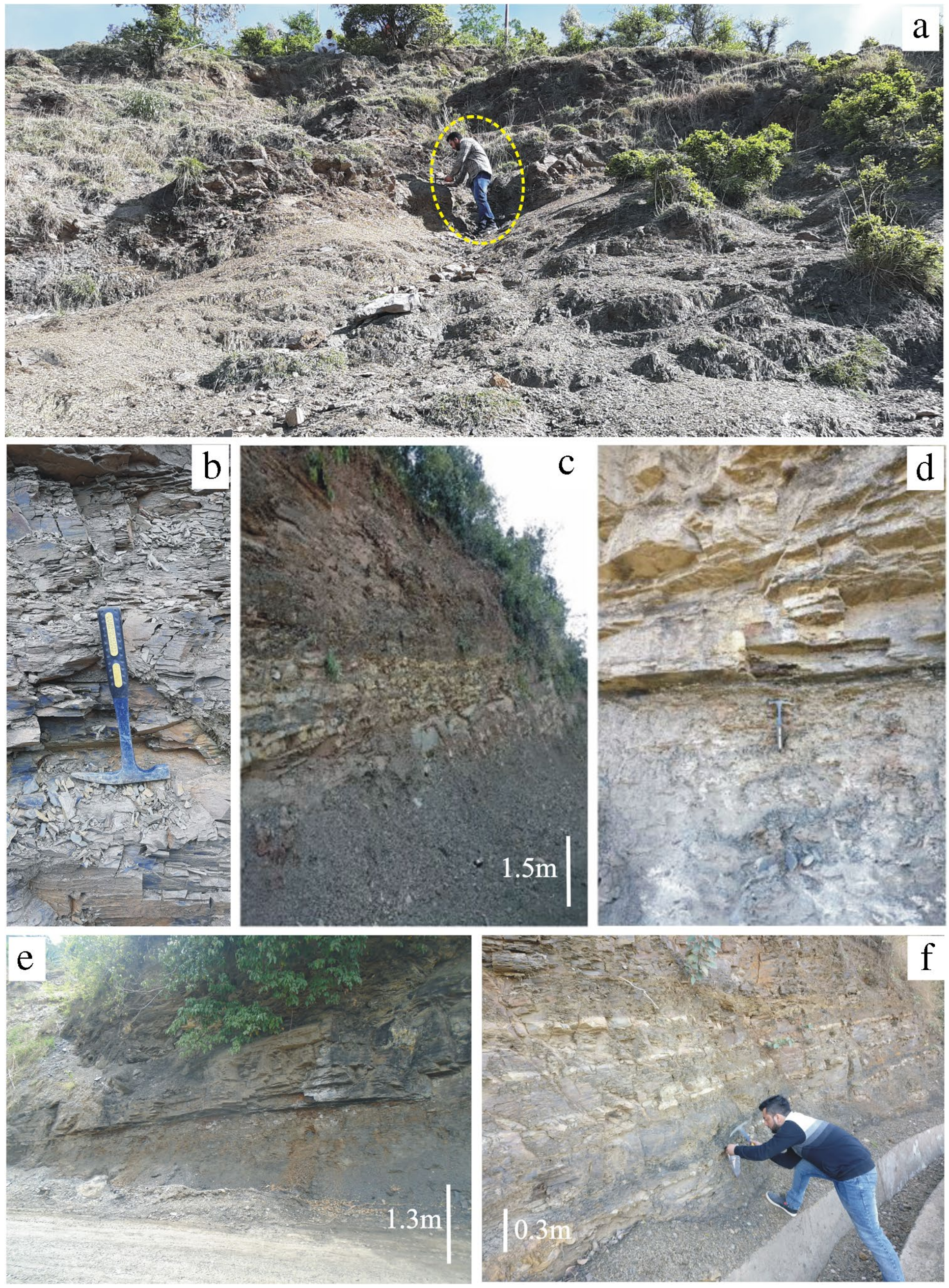

Fig. 4 Representative field photographs showing characteristic sedimentary facies of OAE in the Paleocene-Eocene dated Subathu Formation exposed in and around the Kalakot area of Jammu and Kashmir (India). Facies present includes black to gray shale in alteration with coal and siltstone/fossiliferous limestone. Person and geological hammer used as scale are, respectively, ~180 and ~29 cm. Photographs comprise both inclined (i.e., a and e) and sub-vertical to vertical (i.e., b, c, d, and f) surfaces

can be broadly subdivided into the Paleogene Pre-Siwalik sediments and the Neogene Siwalik Group sediments. The Paleocene-Middle Eocene marine transgression commenced with deposition of the Subathu Formation and its age has been estimated to range between 61.5 and 43.7 Ma (Lakshami et al. 2000), whereas Sangode et al. (2005) magnetostratigraphically dated its uppermost part as ~41.5 Ma. The Subathu Formation is the oldest (Paleocene-Eocene) stratigraphic unit of HFB and predominately consists of fossiliferous marine limestone and shale. Its deposition started well before the Himalayan upheaval as it has minimal evidence of terrigenous clastic influence. The shallow marine Subathu Formation predominantly consists of shale with siltstone, thin fossiliferous limestone, and sandstone intercalations (Raiverman, 1979) and is deposited during the initial phase of contact, collision, and shutters. It overlies the Precambrian Simla Slates in Himachal Pradesh and Sirban Limestone in Jammu and Kashmir and is overlain by the continental deposits of the Murree Group (equivalent to Dagshai and Kasauli Formations/Dharamsala Formation in different parts of the HFB). These marines to shallow marine, regionally extensive, black to gray-green shales represent last phase deposits of the Tethys Sea. These coincide

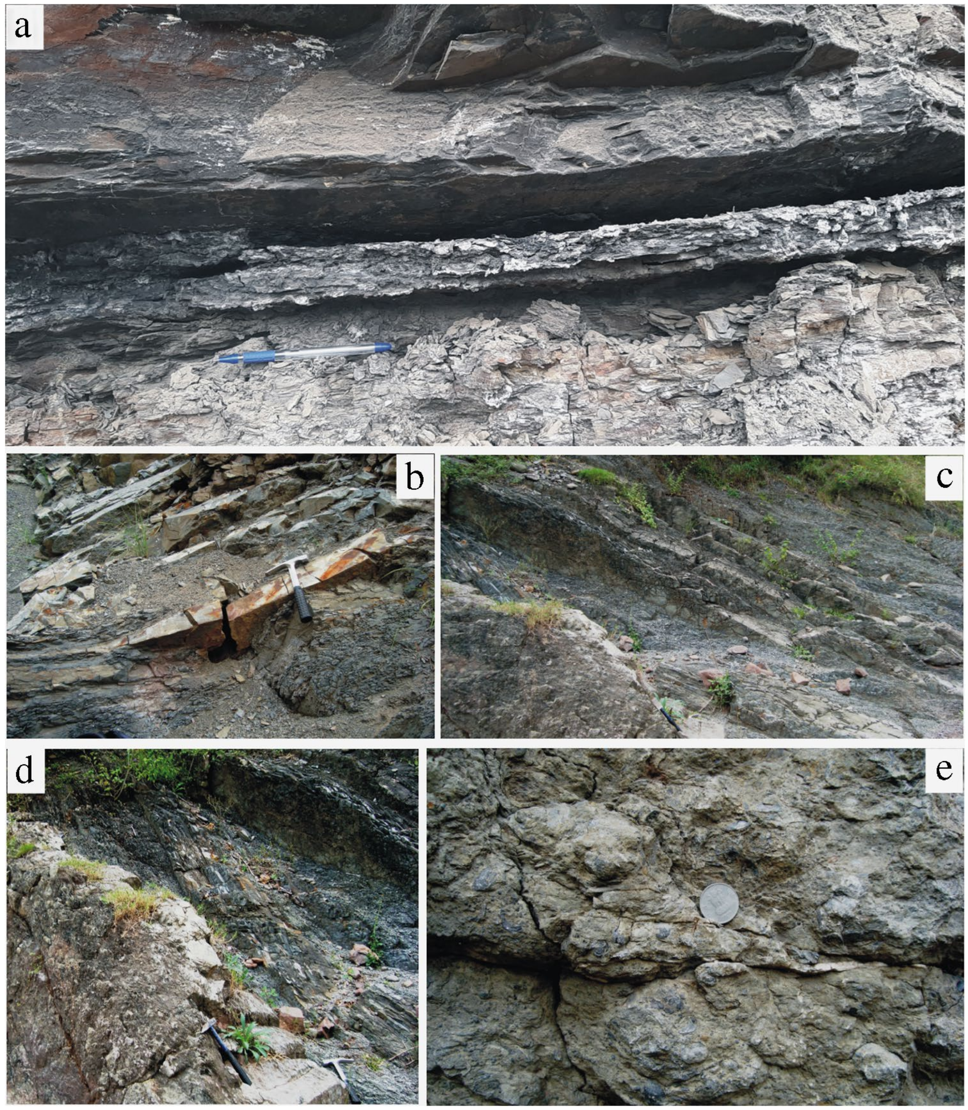

Fig. 5 Representative field photographs showing characteristic sedimentary facies of OAE in the Paleocene-Eocene dated Subathu Formation exposed **a** in and around Jammu region of Jammu and Kashmir (India) and the photograph is of sub-vertical surface (**b**) to **e** in and around Koti area of Simla hills in the Himachal Pradesh state of India. An alternating sequence of black to grayish green shale, fossiliferous limestone, and siltstone are present. The geological hammer used as the scale is ~29 cm. Photographs b and c are of inclined surfaces. Photographs d and e are closer views of c to show biofacies/fossils

with PETM and require detailed investigations because these may represent records of Paleocene-Eocene OAE.

Thus, Paleocene-Eocene HFB marine sediments represented by Subathu Formation (Patala and Balakot formations) occur in and around the Jammu region (of the Ramnagar sub-basin) and Simla region (of the Subathu sub-basin) and have been explored for sedimentary facies indicative of anoxic conditions. Representative field photographs are shown in Figs. 4 and 5. These comprise alternating sequences of calcareous and argillaceous sediments. In general, breccia, bauxite, coal and black, carbonaceous shale occur in the basal part of the succession followed by alternations of shale and marl. This formation has yielded various shallow marine invertebrate fossils, particularly foraminifers. Some of the shale beds are referred to as nummulitic shales due to an abundance of these fossils. Acharyya (2007) reported that Mathur and Juyal (2000) showed the presence of *Daviesina gurumensis* of late Thanetinian age from the basal Subathu Formation with pisolitic laterite from this Kalakot section of the Jammu region. Calculated TOC values from representative black, gray to green shales range 0.1 to 4.2%. The Subathu Formation is considered a principal transgressive-regressive succession that incorporates a rhythmic series of small-scale repetitions, wherein limestones represent transgressions and shales represent regressions (Singh and Andotra 2000). Thus, lithofacies association in Subathu Formation shows alternating transgressive and regressive facies. Chaudhri (1976) recognized three transgressive and regressive cycles. As discussed under Section Eustatic sea level *change*, such transgression and regression phases are commonly associated with OAEs.

Therefore, these early (i.e., Paleocene-Eocene) Himalayan foreland basin sediments deposited under marginal marine, euxinic conditions on the basis of above-documented lithofacies and contain sufficient TOC amount. This kind of depositional environment for these sediments has been well established by other researchers all along the HFB. It suggests the possible representation of these early Himalayan sediments as records of OAE. For example, the very first and foremost OAE indicator is the presence of characteristic sedimentary and biostratigraphic facies (Section Characteristics of oceanic anoxic events (OAEs)) shown by them. These Paleocene-Eocene Himalayan sediments are laterally extensive all along the HFB and the Subathu Formation occurs in discontinuous fragments along the flanks of the Sirban Limestone's Inliers and varies in thickness. The thickness observed at an outcrop in and around the Kalakot area (Jammu region) is about 5080 m. The exact thickness of this formation is complex due to the tectonic complexity of the region. Thus, extensive studies all along the HFB covering these marines to shallow marine Paleocene-Eocene Himalayan foreland basin sediments in the context of anoxic events is overdue to establish records of the spatial extent of OAE in these sediments.

Conclusions

This comprehensive review shows that enormous work on OAEs has been done worldwide. However, more studies on OAEs in parts of India require attention. Also, a review of various major factors for identified OAEs as given by researchers throughout geological history suggest that the regional to global scale OAEs occurred in shallow marine sediments during rapid, persistent greenhouse/hyperthermal (i.e., global warming) state of the Earth. This is irrespective of the factors responsible for this state of Earth. For example, the Mesozoic Era represents the greenhouse state, and substantial evidence of rapid global warming during Jurassic and Cretaceous time periods have been reported, wherein maximum numbers of OAEs have been identified.

The Paleocene-Eocene epoch of the Cenozoic represents the only identified OAE in the Cenozoic Era (i.e., PETM) by some researchers as these remarkably share features similar to those of Paleozoic and Mesozoic OAEs. However, the coeval Paleocene-Eocene dated early HFB sediments deposited during the closing of Tethys Sea have not been studied in detail for OAE records irrespective of their good geological exposures all along the HFB. Such exposures in and around the Jammu region and Simla region represented by Subathu Formation have shown OAE specific bio- and litho-facies associations which are characteristic of alternating transgressive-regressive successions. Deposition of these sediments, comprising dominantly the black to gray-green shales took place under euxinic, shallow marine conditions but occur in discontinuous patches all along the HFB and also greatly vary in thickness due to the tectonic complexity of the Himalayan region. Perhaps the tectonic complexity of the Himalayan region and discontinuous occurrence of these regionally extensive early HFB sediments is the reason behind their meager studies. Nevertheless, these sediments representing the last phase deposits of the Tethys Sea during PETM, need extensive investigations all along the HFB because these could reveal at least a regional, if not global scale OAE during Paleocene-Eocene time of Himalayan orogeny.

Supplementary Information The online version contains supplementary material available at https://doi.org/10.1007/s12517-021-09180-y.

Acknowledgements We thank the Department of Geology (Panjab University, Chandigarh, India) and the Department of Petroleum Engineering and Earth Sciences (University of Petroleum and Energy Studies, Dehradun, India) for providing necessary facilities. The first author is grateful to mentors/doctorate supervisors (Seema Singh and Uday Bhan) and Council of Scientific and Industrial Research (India) for providing the research fellowship, grant no. 09/135(0732)/2015EMR-1. We greatly appreciate and thank the Editor, one anonymous reviewer, and another reviewer, Prof. Soumyajit Mukherjee (IIT Bombay) for their constructive comments and suggestions that helped improve this article.

Declarations

Conflict of interest The authors declare no competing interests.

References

Acharyya SK (2007) Evolution of the Himalayan Paleogene foreland basin, influence of its litho-packet on the formation of thrust-related domes and windows in the Eastern Himalayas–a review. J Asian Earth Sci 31(1):1–17

Algeo TJ, Maynard JB (2004) Trace-element behavior and redox facies in core shales of upper Pennsylvanian Kansas-type cyclothems. Chem Geol 206(3-4):289–318

Al-Sagri KEA (2015) Linking the timing of deposition and organic matter richness of the Gulneri formation of Northern Iraq to the global oceanic anoxic event 2 (OAE 2): implications to better constrain the depositional models of Iraqi's oil source beds and their timing of deposition. Iraq J Sci 56(3A):2007–2023

Al-Suwaidi AH, Angelozzi GN, Baudin F, Damborenea SE, Hesselbo SP, Jenkyns HC, Manceñido MO, Riccardi AC (2010) First record of the early Toarcian oceanic anoxic event from the southern hemisphere, Neuquén Basin, Argentina. J Geol Soc 167(4):633–636

Alvarez LW, Alvarez W, Asaro F, Michel HV (1980) Extraterrestrial cause for the Cretaceous-Tertiary extinction. Science 208(4448):1095–1108

Andjić G, Baumgartner PO, Baumgartner-Mora C (2018) Rapid vertical motions and formation of volcanic arc gaps: plateau collision recorded in the forearc geological evolution (Costa Rica margin). Basin Res 30(5):863–894

Arora A, Banerjee S, Dutta S (2015) Black shale in late Jurassic Jhuran formation of Kutch: possible indicator of oceanic anoxic event. J Geol Soc India 85(3):265–278

Arthur MA, Sageman BB (1994) Marine black shales: depositional mechanisms and environments of ancient deposits. Annu Rev Earth Planet Sci 22(1):499–551

Arthur MA, and Sageman BB, (2005). Sea level control on source rock development: perspectives from the Holocene Black Sea, the mid-Cretaceous Western interior basin of North America, and the Late Devonian Appalachian basin: SEPM special publication No. 82. in Harris NB (ed.), the deposition of organic carbon-rich sediments: models, mechanisms and consequences: SEPM special publication No. 82.

Arthur MA, Schlanger SO (1979) Cretaceous “oceanic anoxic events” as causal factors in development of reef-reservoired giant oil fields. AAPG Bull 63(6):870–885

Arthur MA, Dean WE, Schlanger SO (1985) Variations in the global carbon cycle during the Cretaceous related to climate, volcanism, and changes in atmospheric CO2. The carbon cycle and atmospheric CO2: natural variations. Archean Present 32:504–529

Arthur MA, Schlanger ST, Jenkyns HC (1987) The Cenomanian-Turonian oceanic anoxic event, II. Palaeoceanographic controls on organic-matter production and preservation. Geol Soc, London, Special Publications 26(1):401–420

Arthur MA, Jenkyns HC, Brumsack HJ, Schlanger SO (1990) In: Ginsburg RN, Beaudoin B (eds) Stratigraphy, geochemistry, and paleoceanography of organic carbon rich Cretaceous sequences, in Cretaceous resources, events and rhythms, NATO ASI Ser, 304th edn. Kluwer Acad, Dordrecht, pp 75–119

Barclay J, Herd RA, Edwards BR, Christopher T, Kiddle EJ, Plail M, Donovan A (2010) Caught in the act: implications for the increasing abundance of mafic enclaves during the recent eruptive episodes of the Soufrière Hills volcano, Montserrat. Geophys Res Lett 37(19)

Bailey TR, Rosenthal Y, McArthur JM, van de Schootbrugge B, Thirlwall MF (2003) Paleoceanographic changes of the late Pliensbachian–early Toarcian interval: a possible link to the genesis of an oceanic anoxic event, earth planet. Sci Lett 212:307–320

Bailey TR, Rosenthal Y, McArthur JM, Van de Schootbrugge B, Thirlwall MF (2003) Paleoceanographic changes of the Late Pliensbachian–Early Toarcian interval: a possible link to the genesis of an oceanic anoxic event. Earth Planet Sci Lett *212*(3-4):307–320

Banerjee S, Dutta S, Paikaray S, Mann U (2006) Stratigraphy, sedimentology and bulk organic geochemistry of black shales from the Proterozoic Vindhyan Supergroup (central India). J Earth Syst Sci 115(1):37–47

Bansal U, Pande K, Banerjee S, Nagendra R, Jagadeesan KC (2019) The timing of oceanic anoxic events in the Cretaceous succession of Cauvery basin: constraints from 40Ar/39Ar ages of glauconite in the Karai Shale Formation. Geol J 54(1):308–315

Bansal U, Banerjee S, Ruidas DK, Pande K (2018) Origin and geochemical characterization of Maastrichtian glauconites in the, Central India. J Palaeogeogr 7:99–116

Bartlett R, Elrick M, Wheeley JR, Polyak V, Desrochers A, Asmerom Y (2018) Abrupt global-ocean anoxia during the Late Ordovician–early Silurian detected using uranium isotopes of marine carbonates. Proc Natl Acad Sci 115(23):5896–5901

Barash MS (2012) Causes and prime causes of mass biotic extinctions in the Phanerozoic. In Doklady earth sciences (Vol. 445, no. 2, 925). Springer Nature BV

Barron EJ (1987) Eocene equator-to-pole surface ocean temperatures: a significant climate problem? Paleoceanography 2(6):729–739

Bastos LPH, Pereira E, da Costa Cavalcante D, Alferes CLF, de Menezes CJ, Rodrigues R (2020) Expression of Early Cretaceous global anoxic events in Northeastern Brazilian basins. Cretac Res 110:104390

Baudin F (2005) A Late Hauterivian short-lived anoxic event in the Mediterranean Tethys: the ‘Faraoni event’. ComptesRendus Geosci 337(16):1532–1540

Becker RT (1993) Anoxia, eustatic changes, and upper Devonian to lowermost Carboniferous global ammonoid diversity. Syst Assoc Special 47:115e163

Becker RT, Kirchgasser WT (2007) Devonian events and correlations. The. Geol Soc Spec Publ 278:1e280

Becker L, Poreda RJ, Hunt AG, Bunch TE, Rampino M (2001) Impact event at the Permian-Triassic boundary: evidence from extraterrestrial noble gases in fullerenes. Science 291(5508):1530–1533

Beil S, Kuhnt W, Holbourn A, Scholz F, Oxmann J, Wallmann K, Lorenzen J, Aquit M, Chellai EH (2020) Cretaceous oceanic anoxic events prolonged by phosphorus cycle feedbacks. Clim Past 16(2):757–782

Bernoulli D (1972) North Atlantic and Mediterranean Mesozoic facies: a comparison. Initial Reports of the Deep sea Drilling Project 11:801–871

Bernoulli D, Peters T (1970) Traces of rhyolitic-trachytic volcanism in the upper Jurassic of the Southern Alps. Eclogae Geol Helvetiae 63(2):609–621

Bertle RJ, Suttner TJ (2005) New biostratigraphic data for the Chikkim formation (Cretaceous, Tethyan Himalaya, India). Cretac Res 26(6):882–894

Bhargava ON (2008) An updated introduction to the Spiti geology. J Paleontol Soc India 53(2):113–129

Bhargava ON and Bassi UK, (1998). Geology of Spiti-Kinnaur Himachal Himalaya (124). Geological Survey of India.

Biswas SK (1971) The miliolite rocks of Kutch and Kathiawar (western India). Sediment Geol 5(2):147–164

Biswas SK (1977) Mesozoic rock-stratigraphy of Kutch, Gujarat. Q J Geol Mineral Metall Soc India 49:1–51

Biswas SK, 1980. Structure of Kutch-Kathiawar Region, Western India. In Proc. 3rd Indian Geological Congress, Pune (255-272).

Biswas SK (1981) Basin framework, paleo-environment and depositional history of the Mesozoic sediments of Kutch basin, western India. Q J Geol Min Metall Soc India 53:56–85

Bodin S, Godet A, Matera V, Steinmann P, Vermeulen J, Gardin S, Adatte T, Coccioni R, Föllmi KB (2007) Enrichment of redox-sensitive trace metals (U, V, Mo, As) associated with the late HauterivianFaraoni oceanic anoxic event. Int J Earth Sci 96(2):327–341

Bodin S, Mattioli E, Fröhlich S, Marshall JD, Boutib L, Lahsini S, Redfern J (2010) Toarcian carbon isotope shifts and nutrient changes from the northern margin of Gondwana (high atlas, Morocco, Jurassic): palaeoenvironmental implications. Palaeogeogr Palaeoclimatol Palaeoecol 297(2):377–390

Bodin S, Mattioli E, Fröhlich S, Marshall JD, Boutib L, Lahsini S, Redfern J (2010) Toarcian carbon isotope shifts and nutrient changes from the Northern margin of Gondwana (High Atlas, Morocco, Jurassic): palaeoenvironmental implications. Palaeogeogr Palaeoclimatol Palaeoecol 297(2):377–390

Bohaty SM, Zachos JC, Sluijs A, Gibbs SJ, Brinkhuis H, Bralower TJ (2008) North American continental margin records of the Paleocene–Eocene thermal maximum: implications for global carbon and hydrological cycling. Paleoceanography 23:2217

Bomou B, Adatte T, Tantawy AA, Mort H, Fleitmann D, Huang Y, Föllmi KB (2013) The expression of the Cenomanian–Turonian oceanic anoxic event in Tibet. Palaeogeogr Palaeoclimatol Palaeoecol 369:466–481

Bonacina G, Sanfilippo A, Zana S, Bosino A, Massara EP, Viaggi P et al (2021) Geochemical evidence for local variability in redox and depositional conditions in a deep-water bonarelli equivalent section from southern tethys (fontanavalloneto section, southern italy). Ofioliti 46(1):43–62

Bornemann A, Norris RD, Friedrich O, Eckmann B, Schouten S, Sinninghe Damsté JS, Vogel J, Hofmann P, Wagner T (2008)

Isotopic evidence for glaciation during the Cretaceous super-greenhouse. Science 319:189–192
Bottini C, Mutterlose J (2012) Integrated stratigraphy of Early Aptian black shales in the Boreal Realm: calcareous nannofossil and stable isotope evidence for global and regional processes. Newsl Stratigr 45(2):115–137
Bottini C, Cohen AS, Erba E, Jenkyns HC, Coe AL (2012) Osmium-isotope evidence for volcanism, weathering, and ocean mixing during the early Aptian OAE 1a. Geology 40(7):583–586
Bottjer DJ, Droser ML, Sheehan PM, McGhee GR and Allmon WD, 2001. The ecological architecture of major events in the Phanerozoic history of marine invertebrate life. Evol Paleoecol: The ecological context of macroevolutionary change, 1748.
Boulila S, Hinnov LA (2017) A review of tempo and scale of the early Jurassic Toarcian OAE: implications for carbon cycle and sea level variations. Newsl Stratigr 50(4):363–389
Bralower TJ, Fullagar PD, Paul CK, Dwyer GS, Leckie RM (1997) Mid-Cretaceous strontium-isotope stratigraphy of deep-sea sections. Geol Soc Am Bull 109:1421–1442
Bralower TJ, Sliter WV, Arthur MA, Leckie RM, Allard D, Schlanger SO (1993) Dysoxic/anoxic episodes in the Aptian-Albian (early cretaceous). The Mesozoic Pacific: geology, tectonics, and volcanism 77:5–37
Brassell SC (2009) Steryl ethers in a Valanginian claystone: molecular evidence for cooler waters in the Central Pacific during the early cretaceous? Palaeogeogr Palaeoclimatol Palaeoecol 282(1–4):45–57
Bratton JF (1999) Clathrate eustasy: methane hydrate melting as a mechanism for geologically rapid sea-level fall. Geology 27(10):915–918
Breitburg D, Levin LA, Oschlies A, Grégoire M, Chavez FP, Conley DJ, Garçon V, Gilbert D, Gutiérrez D, Isensee K, Jacinto GS (2018) Declining oxygen in the global ocean and coastal waters. Science 359:6371
Brumsack HJ (2006) The trace metal content of recent organic carbon-rich sediments: implications for Cretaceous black shale formation. Palaeogeogr Palaeoclimatol Palaeoecol 232(2):344–361
Buggisch W (1991a) The global Frasnian-FamennianKellwasser Event. Geol Rundsch 80(1):49–72
Canfield DE, Poulton SW, Knoll AH, Narbonne GM, Ross G, Goldberg T, Strauss H (2008) Ferruginous conditions dominated later Neoproterozoic deep-water chemistry. Science 321(5891):949–952
Carter A, Najman Y, Bahroudi A, Bown P, Garzanti E, Lawrence RD (2010) Locating earliest records of orogenesis in western Himalaya: evidence from Paleogene sediments in the Iranian Makran region and Pakistan Katawaz basin. Geology 38(9):807–810
Cecca F, Fözy I, Wierzbowski A (1993) Ammonites et paléoécologie: Étude quantitative d'associations du Tithonien inférieur de la Téthys occidentale. Geobios 26:39–48
Cecca F, Marini A, Pallini G, Baudin F, Begouen V (1994) A guide-level of the uppermost Hauterivian (Lower Cretaceous) in the pelagic succession of Umbria-Marche Apennines (Central Italy): the FaraoniLevel. RivistaItaliana di paleontologia e Stratigrafia 99(for 1993):551–568
Cecca F, Galeotti S, Coccioni R and Erba E, (1996). the equivalent of the “faraonilevel”(uppermost hauterian, lower cretaceous) recorded in the eastern paret of trento plateau (venetian southern alps, italy).RivistaItaliana di Paleontologia e Stratigrafia, 102(3).
Chaudhri RS (1976) Paleocene-Eocene sequence of northwestern Himalayas-a product of rhythmic sedimentation. Journal of Geological Society of India (Online archive from Vol 1 to Vol 78) 17(1):67–72
Cheng K, Elrick M, Romaniello SJ (2020) Early Mississippian ocean anoxia triggered organic carbon burial and late Paleozoic cooling: evidence from uranium isotopes recorded in marine limestone. Geology 48(4):363–367
Chiarenza AA, Farnsworth A, Mannion PD, Lunt DJ, Valdes PJ, Morgan JV, Allison PA (2020) Asteroid impact, not volcanism, caused the end-Cretaceous dinosaur extinction. Proc Natl Acad Sci 117(29):17084–17093
Coccioni A, Nesci O, Tramontana M, Wezel FC, Moretti E (1987) Descrizione di un livello- guida Radiolaritico-bituminosoittiolit-icoalla base dellemarne a fucoidinell 'Appenninoumbro- marchigiano. BollettinodellaSocietaGeologica Italiana 106(1):183–192
Coccioni R, Bancalà G, Catanzarit R, Fornaciari E, Frontalini F, Giusberti L, Jovane L, Luciani V, Savian J, Sprovieri M (2012) An integrated stratigraphic record of the Palaeocene–lower Eocene at Gubbio (Italy): new insights into the early Palaeogene hyperthermals and carbon isotope excursions. Terra Nova 24(5):380–386
Cohen AS, Coe AL, Harding SM, Schwark L (2004) Osmium isotope evidence for the regulation of atmospheric CO2 by continental weathering. Geology 32(2):157–160
Cohen AS, Coe AL, Kemp DB (2007) The Late Palaeocene–Early Eocene and Toarcian (Early Jurassic) carbon isotope excursions: a comparison of their time scales, associated environmental changes, causes and consequences. J Geol Soc 164(6):1093–1108
Coleman DS, Glazner AF (1997) The sierra crest magmatic event: rapid formation of juvenile crust during the late cretaceous in California. Int Geol Rev 39(9):768–787
Colman, A. S., and Holland, H. D., 2000. The global diagenetic flux of phosphorus from marine sediments to the oceans: redox sensitivity and the control of atmospheric oxygen levels.
Courtillot V (2002) Evolutionary catastrophes: the science of mass extinction. Cambridge University Press
Courtillot VE, Renne PR (2003) On the ages of flood basalt events. Compt Rendus Geosci 335(1):113–140
Cronin TM, Hayo K, Thunell RC, Dwyer GS, Saenger C, Willard DA (2010) The medieval climate anomaly and little ice age in Chesapeake Bay and the North Atlantic Ocean. Palaeogeogr Palaeoclimatol Palaeoecol 297(2):299–310
De Wit MJ, Ghosh JG, de Villiers S, Rakotosolofo N, Alexander J, Tripathi A, Looy C (2002) Multiple organic carbon isotope reversals across the Permo-Triassic boundary of terrestrial Gondwana sequences: clues to extinction patterns and delayed ecosystem recovery. J Geol 110(2):227–240
Demaison GJ, Moore GT (1980) Anoxic environments and oil source bed genesis. Org Geochem 2(1):9–31
Denise B, Levin Lisa A, Andreas O, Marilaure G, Chavez Francisco P, Conley Daniel J, Véronique G, Denis G, Dimitri G, Kirsten I, Jacinto Gil S (2018) Declining oxygen in the global ocean and coastal waters. Science 359(6371):10–1126
Dera G, Donnadieu Y (2012) Modeling evidences for global warming, Arctic seawater freshening, and sluggish oceanic circulation during the Early Toarcian anoxic event. Paleoceanography 27(2):PA2211
Dickens GR (2001) The potential volume of oceanic methane hydrates with variable external conditions. Org Geochem 32(10):1179–1193
Dickens GR (2011) Down the rabbit hole: toward appropriate discussion of methane release from gas hydrate systems during the Paleocene-Eocene thermal maximum and other past hyperthermal events. Clim Past 7(3):831–846
Dickens GR, O'Neil JR, Rea DK, Owen RM (1995) Dissociation of oceanic methane hydrate as a cause of the carbon isotope excursion at the end of the Paleocene. Paleoceanography 10(6):965–971
Du Vivier AD, Selby D, Sageman BB, Jarvis I, Gröcke DR, Voigt S (2014) Marine 187 Os/188 Os isotope stratigraphy reveals the interaction of volcanism and ocean circulation during oceanic anoxic event 2. Earth Planet Sci Lett 389:23–33
Duchamp-Alphonse S, Fiet N, Adatte T, Pagel M (2011) Climate and sea-level variations along the northwestern Tethyan margin

during the Valanginian C-isotope excursion: mineralogical evidence from the Vocontian Basin (SE France). Palaeogeogr Palaeoclimatol Palaeoecol 302(3-4):243–254

Dumitrescu M, Brassell SC, Schouten S, Hopmans EC, Damsté JSS (2006) Instability in tropical Pacific sea-surface temperatures during the early Aptian. Geology 34(10):833–836

Dumitrescu M, Brassell SC (2006) Compositional and isotopic characteristics of organic matter for the early Aptian oceanic anoxic event at Shatsky Rise, ODP Leg 198. Palaeogeogr Palaeoclimatol Palaeoecol 235:168– 191. https://doi.org/10.1016/j.palaeo.2005.09.028. CrossrefWeb of Science®Google Scholar

Dutta D, Mukherjee S (2019) Opposite shear senses: geneses, global occurrences, numerical simulations and a case study from the Indian western Himalaya. J Struct Geol 126:357–392

Duque-Botero F, Maurrasse FJR, Hickey-Vargas R, Melinte MC, Jaffe R, López-Oliva JG (2009) Microspheroid accumulations and geochemical characteristics of a Cenomanian–Turonian anoxic basin: the record of the Indidura formation, NE México: geologic problem solving with microfossils: a volume in honor of Garry D. Jones, Society of Economic Paleontologists and Mineralogists. Special Publ 93:171–186

El Asmi, K., Soussi, M., Ismail, H.B., Hantzpergue, P., Enay, R., and Mangold, C., 2003. Mesozoic sedimentary record of Southern Tunisia and sea-lavel change–the Late Callovian Ghomrassen carbonate platform. In 1st EAGE North African/Mediterranean Petroleum & Geosciences Conference & Exhibition (pp. cp-8). European Association of Geoscientists & Engineers.

Eldrett JS, Minisini D, Bergman SC (2014) Decoupling of the carbon cycle during ocean anoxic event 2. Geology 42(7):567–570

Erbacher J, Friedrich O, Wilson PA, Birch H, Mutterlose J (2005) Stable organic carbon isotope stratigraphy across oceanic anoxic event 2 of demerara rise, western tropical Atlantic. Geochem Geophys Geosyst 6(6)

Erba E (2004) Calcareous nannofossils and Mesozoic oceanic anoxic events. Mar Micropaleontol 52(1):85–106

Erba E, Bartolini A, Larson RL (2004) ValanginianWeissert oceanic anoxic event. Geology 32(2):149–152

Erbacher J, Huber BT, Norris RD, Markey M (2001) Increased thermohaline stratification as a possible cause for an ocean anoxic event in the Cretaceous period. Nature 409(6818):325–327

Elrick M, Berkyová S, Klapper G, Sharp Z, Joachimski M, Frýda J (2009) Stratigraphic and oxygen isotope evidence for my-scale glaciation driving eustasy in the early–middle Devonian greenhouse world. Palaeogeogr Palaeoclimatol Palaeoecol 276(1–4):170–181

Ernst RE, Youbi N (2017) How large igneous provinces affect global climate, sometimes cause mass extinctions, and represent natural markers in the geological record. Palaeogeogr Palaeoclimatol Palaeoecol 478:30–52

Fantasia A, Föllmi KB, Adatte T, Bernárdez E, Spangenberg JE, Mattioli E (2018) The Toarcian oceanic anoxic event in southwestern Gondwana: an example from the Andean basin, northern Chile. J Geol Soc 175(6):883–902

Farrimond P, Talbot HM, Watson DF, Schulz LK, Wilhelms A (2004) Methylhopanoids: molecular indicators of ancient bacteria and a petroleum correlation tool. Geochim Cosmochim Acta 68(19):3873–3882

Fauré P, Peybernès B (1986) Biozonation par Ammonites et essai de corrélation des séries réduites liasiques de la Dorsale Tunisiennë. Bull de la Soc d'histoire Nat Toulouse 122:41–49

Fleurance S, Cuney M, Malartre F, Reyx J (2013) Origin of the extreme polymetallic enrichment (Cd, Cr, Mo, Ni, U, V, Zn) of the Late Cretaceous–Early Tertiary Belqa Group, central Jordan. Palaeogeogr Palaeoclimatol Palaeoecol 369:201–219

Forster A, Schouten S, Baas M, SinningheDamsté JS (2007) Mid-Cretaceous (Albian–Santonian) sea surface temperature record of the tropical Atlantic Ocean. Geology 35(10):919–922

Főzy I, Janssen NM, Price GD, Knauer J, Pálfy J (2010) Integrated isotope and biostratigraphy of a lower Cretaceous section from the Bakony Mountains (Transdanubian Range, Hungary): a new Tethyan record of the Weissert event. Cretac Res 31(6):525–545

Frakes LA, Francis JE, Syktus JI (1992) Climate modes of the Phanerozoic (286)

Freeman KH, Hayes JM (1992) Fractionation of carbon isotopes by phytoplankton and estimates of ancient CO2 levels. Glob Biogeochem Cycles 6(2):185–198

French KL, Sepúlveda J, Trabucho-Alexandre J, Gröcke DR, Summons RE (2014) Organic geochemistry of the early Toarcian oceanic anoxic event in Hawsker Bottoms, Yorkshire, England. Earth Planet Sci Lett 390:116–127

Friedrich O, Norris RD, Erbacher J (2012) Evolution of middle to late cretaceous oceans—a 55 my record of Earth's temperature and carbon cycle. Geology 40(2):107–110

Gale AS, Jenkyns HC, Kennedy WJ, Corfield RM (1993) Chemostratigraphy versus biostratigraphy: data from around the Cenomanian–Turonian boundary. J Geol Soc 150(1):29–32

Gale AS, Kennedy WJ, Voigt S, Walaszczyk I (2005) Stratigraphy of the upper Cenomanian–Lower Turonian chalk succession at Eastbourne, Sussex, UK: ammonites, inoceramid bivalves and stable carbon isotopes. Cretac Res 26(3):460–487

Ganguly S, Tiwari S, Bhan U, Mittal S, Rai S, Osta EF (2015) Melting of sea ice inexplicable for recent global eustatic sea level rise. J Earth Sci Clim Change *6*(1):1

Godet A, Hfaiedh R, Arnaud-Vanneau A, Zghal I, Arnaud H, Ouali J (2014) Aptian palaeoclimates and identification of an OAE1a equivalent in shallow marine environments of the southern Tethyan margin: evidence from Southern Tunisia (Bir Oum Ali section, Northern Chott Chain). Cretac Res 48:110–129

Griesbach CL (1889) Geology of the central Himalayas. Memoirs Geol Survey India 23:1–232

Gröcke DR, Hesselbo SP, Jenkyns HC (1999) Carbon-isotope composition of Lower Cretaceous fossil wood: Ocean-atmosphere chemistry and relation to sea-level change. Geology 27(2):155–158

Gröcke DR, Hori RS, Trabucho-Alexandre J, Kemp DB, Schwark L (2011) An open ocean record of the Toarcian oceanic anoxic event. Solid Earth 2(2):245–257

Hallam A (1994) Strontium isotope profiles of Triassic-Jurassic boundary sections in England and Austria. Geology 22(12):1079–1082

Hallam A, Bradshaw MJ (1979) Bituminous shales and oolitic ironstones as indicators of transgressions and regressions. J Geol Soc 136(2):157–164

Haq BU (1998) Natural gas hydrates: searching for the long-term climatic and slope-stability records. Geol Soc Lond, Spec Publ 137(1):303–318

Haq BU, Hardenbol J, Vail PR (1987) Chronology of fluctuating sea levels since the Triassic. Science 235(4793):1156–1167

Harries PJ, Little CT (1999) The early Toarcian (early Jurassic) and the Cenomanian–Turonian (late cretaceous) mass extinctions: similarities and contrasts. Palaeogeogr Palaeoclimatol Palaeoecol 154(1–2):39–66

Hasegawa T (2003) Cretaceous terrestrial paleoenvironments of northeastern Asia suggested from carbon isotope stratigraphy: increased atmospheric pCO2-induced climate. J Asian Earth Sci 21(8):849–859

Hay WW (1995) Paleoceanography of marine organic-carbon-rich sediments

Hays JD, Pitman WC (1973) Lithospheric plate motion, sea level changes and climatic and ecological consequences. Nature 246(5427):18–22

He W, Shan X, Sun Y, Cao H, Zheng S, Su S, Kang S (2021) The oil shale formation mechanism of the Songliao Basin Nenjiang Formation triggered by marine transgression and oceanic anoxic events 3. Oil Shale 38(2)

Heath MN, Cramer BD, Stolfus BM, Barnes GL, Clark RJ, Day JE, Barnett BA, Witzke BJ, Hogancamp NJ, Tassier-Surine S (2021) Chemoautotrophy as the driver of decoupled organic and carbonate carbon isotope records at the onset of the Hangenberg (Devonian-Carboniferous Boundary) oceanic anoxic event. Palaeogeogr Palaeoclimatol Palaeoecol 577:110540

Hedges JI, Keil RG (1995) Sedimentary organic matter preservation: an assessment and speculative synthesis. Mar Chem 49(2-3):81–115

Hennekam R, Van der Bolt B, van Nes EH, de Lange GJ, Scheffer M, Reichart GJ (2020) Early-warning signals for marine anoxic events. Geophys Res Lett 47(20):e2020GL089183

Hermoso M, Le Callonnec L, Minoletti F, Renard M, Hesselbo SP (2009) Expression of the Early Toarcian negative carbon-isotope excursion in separated carbonate microfractions (Jurassic, Paris Basin). Earth Planet Sci Lett 277(1):194–203

Hermoso M, Minoletti F, Pellenard P (2013) Black shale deposition during Toarcian super-greenhouse driven by sea level. Clim Past 9(6):2703–2712

Herrle JO, Pross J, Friedrich O, Köbler P, Hemleben C (2003) Forcing mechanisms for mid-Cretaceous black shale formation: evidence from the Upper Aptian and Lower Albian of the Vocontian Basin (SE France). Palaeogeogr Palaeoclimatol Palaeoecol 190:399–426

Herrle JO, Köbler P, Friedrich O, Erlenkeuser H, Hemleben C (2004) High-resolution carbon isotope records of the Aptian to lower Albian from SE France and the Mazagan Plateau (DSDP Site 545): a stratigraphic tool for paleoceanographic and paleobiologic reconstruction. Earth Planet Sci Lett 218(1-2):149–161

Hesselbo SP, Pieńkowski G (2011) Stepwise atmospheric carbon-isotope excursion during the Toarcian oceanic anoxic event (Early Jurassic, Polish Basin). Earth Planet Sci Lett 301(1-2):365–372

Hesselbo SP, Grocke DR, Jenkyns HC, Bjerrum CJ (2000) Massive dissociation of gas hydrate during a Jurassic oceanic anoxic event. Nature 406(6794):392

Hesselbo SP, Jenkyns HC, Duarte LV, Oliveira LC (2007) Carbon-isotope record of the Early Jurassic (Toarcian) oceanic anoxic event from fossil wood and marine carbonate (Lusitanian Basin, Portugal). Earth Planet Sci Lett 253(3):455–470

Heydari E, Hassanzadeh J (2003) Deev Jahi model of the Permian-Triassic boundary mass extinction: a case for gas hydrates as the main cause of biological crisis on Earth. Sediment Geol 163(1–2):147–163

Heydari E, Hassanzadeh J, Wade WJ, Ghazi AM (2003) Permian–Triassic boundary interval in the Abadeh section of Iran with implications for mass extinction: part 1–sedimentology. Palaeogeogr Palaeoclimatol Palaeoecol 193(3-4):405–423

Higgins JA, Schrag DP (2006) Beyond methane: towards a theory for the Paleocene–Eocene thermal maximum. Earth Planet Sci Lett 245(3):523–537 http://www.stratigraphy.org/ICSchart/ChronostratChart2017-02.jpg

Higgins MB, Robinson RS, Husson JM, Carter SJ, Pearson A (2012) Dominant eukaryotic export production during ocean anoxic events reflects the importance of recycled NH4+. Proc Natl Acad Sci 109(7):2269–2274

Hildebrand, A.R., Penfield, G.T., Kring, D.A., Pilkington, M., Camargo Z, A., Jacobsen, S.B. and Boynton, W.V., 1991. Chicxulub crater: a possible cretaceous/tertiary boundary impact crater on the Yucatan peninsula, Mexico. Geology, 19(9), 867–871

Hu X, Zhao K, Yilmaz IO, Li Y (2012) Stratigraphic transition and palaeoenvironmental changes from the Aptian oceanic anoxic event 1a (OAE1a) to the oceanic red bed 1 (ORB1) in the Yenicesihlar section, central Turkey. Cretac Res 38:40–51

Hu G, Hu W, Cao J, Yao S, Liu W, Zhou Z (2014) Fluctuation of organic carbon isotopes of the lower Cretaceous in coastal southeastern China: terrestrial response to the oceanic anoxic events (OAE1b). Palaeogeogr Palaeoclimatol Palaeoecol 399:352–362

Huang C, Hesselbo SP (2014) Pacing of the Toarcian oceanic anoxic event (Early Jurassic) from astronomical correlation of marine sections. Gondwana Res 25(4):1348–1356

Huber BT, Norris RD, MacLeod KG (2002) Deep-sea paleotemperature record of extreme warmth during the Cretaceous. Geology 30(2):123–126

Hutton T (1841) Geological report on the Valley of the Spiti, and the route from Katghur. J Asiat Soc Bengal 10:198–229

Ingall ED, Bustin RM, Van Cappellen P (1993) Influence of water column anoxia on the burial and preservation of carbon and phosphorus in marine shales. Geochim Cosmochim Acta 57(2):303–316

Ingram BL, Coccioni R, Montanari A, Richter FM (1994) Strontium isotopic composition of mid-Cretaceous seawater. Science 264(5158):546–550

Izumi K, Miyaji T, Tanabe K (2012) Early Toarcian (Early Jurassic) oceanic anoxic event recorded in the shelf deposits in the northwestern Panthalassa: evidence from the Nishinakayama formation in the Toyora area, west Japan. Palaeogeogr Palaeoclimatol Palaeoecol 315:100–108

Jain AK, Lal N, Sulemani B, Awasthi AK, Singh S, Kumar R, Kumar D (2009) Detritalzircon fission-track ages from the lower Cenozoic sediments, NW Himalayan foreland basin: clues for exhumation and denudation of the Himalaya during the India-Asia collision. Geol Soc Am Bull 121(3-4):519–535

Jahren AH, Arens NC, Sarmiento G, Guerrero J, Amundson R (2001) Terrestrial record of methane hydrate dissociation in the early cretaceous. Geology 29(2):159–162

Jarvis IAN, Gale AS, Jenkyns HC, Pearce MA (2006) Secular variation in late cretaceous carbon isotopes: a new δ13C carbonate reference curve for the Cenomanian–Campanian (99.6–70.6 ma). Geol Mag 143(5):561–608

Jarvis I, Lignum JS, Gröcke DR, Jenkyns HC, Pearce MA (2011) Black shale deposition, atmospheric CO2 drawdown, and cooling during the Cenomanian-Turonian oceanic anoxic event. Paleoceanography 26(3):PA3201

Jenkyns HC (1980) Cretaceous anoxic events: from continents to oceans. J Geol Soc 137(2):171–188

Jenkyns HC (1985) The Early Toarcian and Cenomanian-Turonian anoxic events in Europe: comparisons and contrasts. Geol Rundsch 74(3):505–518

Jenkyns, H., 1988. The early Toarcian (Jurassic) anoxic event-stratigraphic, sedimentary, and geochemical evidence. American Journal of Science, 288(2), 101-151

Jenkyns HC, (1999).

Jenkyns HC (2003) Evidence for rapid climate change in the Mesozoic–Palaeogene greenhouse world. Philos Trans R Soc London, Ser A 361(1810):1885–1916

Jenkyns HC (2010) Geochemistry of oceanic anoxic events. Geochem Geophys Geosyst 11(3):Q03004

Jenkyns HC (2018) Transient cooling episodes during Cretaceous oceanic anoxic events with special reference to OAE 1a (Early Aptian). Philos Trans R Soc A Math Phys Eng Sci 376(2130):20170073

Jenkyns HC, Clayton CJ (1997) Lower Jurassic epicontinental carbonates and mudstones from England and Wales: chemostratigraphic signals and the early Toarcian anoxic event. Sedimentology 44(4):687–706

Jenkyns HC, Forster A, Schouten S, Damsté JSS (2004) High temperatures in the Late Cretaceous Artic Ocean. Nature 432(7019):888

Jenkyns HC, Dickson AJ, Ruhl M, Boorn SH (2017) Basalt-seawater interaction, the Plenus Cold Event, enhanced weathering and geochemical change: deconstructing Oceanic Anoxic Event 2 (Cenomanian–Turonian, Late Cretaceous). Sedimentology 64(1):16–43

Jiang G, Sohl LE, Christie-Blick N (2003) Neoproterozoic stratigraphic comparison of the lesser Himalaya (India) and Yangtze block (South China): Paleogeographic implications. Geology 31(10):917–920

JIN MS, WANG H, QIAO GB, ZHANG SP (2014) The discovery of Heiqia iron mineralization belt in West Kunlun by high resolution remote sensing technology and its geological significance. Northwest Geol 47(4):221–226

John CM, BohatyJenkyns HC (1999) Mesozoic anoxic events and palaeoclimate. ZentralblattfürGeologie und Paläontologie 1997(7–9):943–949

Jones CE, Jenkyns HC (2001) Seawater strontium isotopes, oceanic anoxic events, and seafloor hydrothermal activity in the Jurassic and Cretaceous. Am J Sci 301(2):112–149

Jones CE, Jenkyns HC, Coe AL, Stephen HP (1994) Strontium isotopic variations in Jurassic and cretaceous seawater. Geochim Cosmochim Acta 58(14):3061–3074

Joo YJ, Sageman BB (2014) Cenomanian to Campanian carbon isotope chemostratigraphy from the Western Interior Basin, USA. J Sediment Res 84(7):529–542

Joo YJ, Sageman BB, Hurtgen MT (2020) Data-model comparison reveals key environmental changes leading to Cenomanian-Turonian Oceanic Anoxic Event 2. Earth Sci Rev 203:103123

Kabanov P (2019) Devonian (c. 388–375 Ma) Horn River Group of Mackenzie Platform (NW Canada) is an open-shelf succession recording oceanic anoxic events. J Geol Soc 176(1):29–45

Kabanov P, Jiang C (2020) Photic-zone euxinia and anoxic events in a middle-late Devonian shelfal sea of Panthalassan continental margin, NW Canada: changing paradigm of Devonian Ocean and sea level fluctuations. Glob Planet Chang 188:103153

Kaiho K (1994) Benthic foraminiferal dissolved-oxygen index and dissolved-oxygen levels in the modern ocean. Geology 22(8):719–722

Kaiho K, Oshima N (2017) Site of asteroid impact changed the history of life on earth: the low probability of mass extinction. Sci Rep 7(1):1–12

Kaiho K, Oshima N, Adachi K, Adachi Y, Mizukami T, Fujibayashi M, Saito R (2016) Global climate change driven by soot at the K-Pg boundary as the cause of the mass extinction. Sci Rep 6(1):1–13

Karakitsios V, Kafousia N, Tsikos H (2010) A review of oceanic anoxic events as recorded in the Mesozoic sedimentary record of mainland Greece. Hellenic J Geosci 45:123

Kassem AA, Sharaf LM, Baghdady AR, El-Naby AA (2020) Cenomanian/Turonian oceanic anoxic event 2 in October oil field, central Gulf of Suez, Egypt. J Afr Earth Sci 165:103817

Keller G, Adatte T, Berner Z, Chellai EH, Stueben D (2008) Oceanic events and biotic effects of the Cenomanian-Turonian anoxic event, Tarfaya Basin, Morocco. Cretac Res 29(5–6):976–994

Keller G, Adatte T, Berner Z, Chellai EH, Stueben D (2008) Oceanic events and biotic effects of the Cenomanian-Turonian anoxic event, Tarfaya Basin. Morocco Cretaceous Res 29(5-6):976–994

Keller G, Nagori ML, Chaudhary M, Reddy AN, Jaiprakash BC, Spangenberg JE, Mateo P, Adatte T (2021) Cenomanian-Turonian sea-level transgression and OAE2 deposition in the Western Narmada Basin, India. Gondwana Res 94:73–86

Keller G, Nagori ML, Chaudhary M, Reddy AN, Jaiprakash BC, Spangenberg JE, Mateo P, Adatte T (2021) Cenomanian-Turonian Sea-level transgression and OAE2 deposition in the Western Narmada Basin. India, Gondwana Research

Kemp DB, Selby D, Izumi K (2020) Direct coupling between carbon release and weathering during the Toarcian oceanic anoxic event. Geology 48(10):976–980

Kennedy LA, Russell JK, Kopylova MG (2002) Mantle shear zones revisited: the connection between the cratons and mantle dynamics. Geology 30(5):419–422

Kennett JP, Stott LD (1991) Abrupt deep-sea warming, palaeoceanographic changes and benthic extinctions at the end of the Palaeocene. Nature 353(6341):225–229

Khain VE, Polyakova ID (2010, June) Oceanic anoxic events and global rhythms of endogenic activity during the Phanerozoic history of the Earth. In: In Doklady Earth Sciences, 432, 2 edn. Springer Nature BV, Dordrecht, p 722

Khan S, Kroon D, Wadood B, Ahmad S and Zhou X, (2021). Marine depositional signatures of the Aptian oceanic anoxic events in the Eastern Tethys, Lower Indus Basin, Pakistan Australia J Earth Sci 1-17.

Kidder DL, Worsley TR (2010) Phanerozoic large igneous provinces (LIPs), HEATT (haline euxinic acidic thermal transgression) episodes, and mass extinctions. Palaeogeogr Palaeoclimatol Palaeoecol 295(1-2):162–191

Klemme HD, Ulmishek GF (1991) Effective petroleum source rocks of the world: stratigraphic distribution and controlling depositional factors. AAPG Bull 75(12):1809–1851

Knoll AH, Bambach RK, Canfield DE, Grotzinger JP (1996) Comparative Earth history and Late Permian mass extinction. Science 273(5274):452–457

Kokh SN, Sokol EV, Gustaytis MA (2021) Mercury anomaly in Oligocene–Miocene Maykop Group sediments (Caucasus Continental Collision Zone): mercury hosts, distribution, and sources. Minerals 11(7):751

Kominz MA, (1984). Oceanic ridge volumes and sea-level change-an error analysis.

Krencker FN, Bodin S, Suan G, Heimhofer U, Kabiri L, Immenhauser A (2015) Toarcian extreme warmth led to tropical cyclone intensification. Earth Planet Sci Lett 425:120–130

Krencker FN, Lindström S, Bodin S (2019) A major sea-level drop briefly precedes the Toarcian oceanic anoxic event: implication for Early Jurassic climate and carbon cycle. Sci Rep 9(1):1–12

Krishan J, Pathak DB, Pandey B, Ojha JR (2000) Transgressive sediment intervals in the Late Jurassic of Kachchh, India. Geo Res For 6:331–332

Krishna J (1983) Callovian – Albian Ammonoid Stratigraphy and Paleobiogeography in the Indian subcontinent with special reference to the Tethys Himalayas. Himal Geol 11:43–72

Krishna J (2017) Introduction and Paleogeographic context, previous work, high-resolution scale, magnetochronologic perspective, radiometric scenario, igneous activities, anoxic events and eustatic fluctuations. In: In The Indian Mesozoic Chronicle. Springer, Singapore, pp 1–26

Krishan JP, Pandey DB, B and Ojha J. R. (2000) Transgressive sediment intervals in the late Jurassic of Kachchh. India GeoRes For 6:331–332

Krull ES, Retallack GJ (2000) δ13C depth profiles from paleosols across the Permian-Triassic boundary: evidence for methane release. Geol Soc Am Bull 112(9):1459–1472

Kump LR, Arthur MA (1999) Interpreting carbon-isotope excursions: carbonates and organic matter. Chem Geol 161(1):181–198

Kuroda J, Ogawa NO, Tanimizu M, Coffin MF, Tokuyama H, Kitazato H, Ohkouchi N (2007) Contemporaneous massive subaerial volcanism and late cretaceous Oceanic Anoxic Event 2. Earth Planet Sci Lett 256(1-2):211–223

Kuroyanagi A, Kawahata H, Ozaki K, Suzuki A, Nishi H, Takashima R (2020) What drove the evolutionary trend of planktic foraminifers during the Cretaceous: oceanic anoxic events (OAEs) directly affected it? Mar Micropaleontol 161:101924

Kuypers MM, Blokker P, Erbacher J, Kinkel H, Pancost RD, Schouten S, Damsté JSS (2001) Massive expansion of marine archaea during a mid-Cretaceous oceanic anoxic event. Science 293(5527):92–95

Kuypers MM, Blokker P, Hopmans EC, Kinkel H, Pancost RD, Schouten S, Damsté JSS (2002) Archaeal remains dominate marine organic matter from the early Albian oceanic anoxic event 1b. Palaeogeogr Palaeoclimatol Palaeoecol 185(1-2):211–234

Kuypers MM, van Breugel Y, Schouten S, Erba E, Damsté JSS (2004) N2-fixing cyanobacteria supplied nutrient N for Cretaceous oceanic anoxic events. Geology 32(10):853–856

Lakshami KJP, Sudheer Kumar M, Bhalla MS, Rao GVSP (2000) Magnetostratigraphy of Himalayan sediments from Himachal Pradesh. J Indian Geophysical Union 4(2):147–154

Lamolda MA, Mao S (1999) The Cenomanian–Turonian boundary event and dinocyst record at Ganuza (northern Spain). Palaeogeogr Palaeoclimatol Palaeoecol 150(1–2):65–82

Langsford N, Raimondo T, Jago J (2020) Red crust: evidence for an early Paleozoic oceanic anoxic event. Aust J Earth Sci 67(7):995–1001

Weissert H (1989) C-isotope stratigraphy, a monitor of paleoenvironmental change: A case study from the Early Cretaceous: Surveys in Geophysics (10:1–61)

Large RR, Halpin JA, Lounejeva E, Danyushevsky LV, Maslennikov VV, Gregory D, Sack PJ, Haines PW, Long JA, Makoundi C, Stepanov AS (2015) Cycles of nutrient trace elements in the Phanerozoic Ocean. Gondwana Res *28*(4):1282–1293

Larson RL (1991) Latest pulse of Earth: evidence for a mid-Cretaceous superplume. Geology *19*(6):547–550

Larson RL, PITMAN III, W.C. (1972) World-wide correlation of Mesozoic magnetic anomalies, and its implications. Geol Soc Am Bull 83(12):3645–3662

Larson RL, Erba E (1999) Onset of the Mid-Cretaceous greenhouse in the Barremian-Aptian: igneous events and the biological, sedimentary, and geochemical responses. Paleoceanography 14(6):663–678

Leckie RM, Bralower TJ, Cashman R (2002) Oceanic anoxic events and plankton evolution: biotic response to tectonic forcing during the mid-Cretaceous. Paleoceanography 17:13-1–13-29

Lehmann J, Friedrich O, Von Bargen D, Hemker T (2012) Early Aptian Bay deposits at the southern margin of the Lower Saxony Basin: integrated stratigraphy, palaeoenvironment and OAE 1a. Acta Geol Pol 62(1):35–62

Lenniger M, Nøhr-Hansen H, Hills LV, Bjerrum CJ (2014) Arctic black shale formation during Cretaceous oceanic anoxic event 2. Geology 42(9):799–802

Li X, Wei Y, Li Y, Zhang C (2016) Carbon isotope records of the early Albian oceanic anoxic event (OAE) 1b from eastern Tethys (southern Tibet, China). Cretac Res 62:109–121

Li X, Jenkyns HC, Wang C, Hu X, Chen X, Wei Y, Huang Y, Cui J (2006) Upper cretaceous carbon and oxygen-isotope stratigraphy of hemipelagic carbonate facies from southern Tibet, China. J Geol Soc 163(2):375–382

Li Y-X, Bralower TJ, Montañez IP, Osleger DA, Arthur MA, Bice DM, Herbert TD, Erba E, Premoli Silva I (2008) Toward an orbital chronology for the early Aptian oceanic anoxic event (OAE1a, ~120 ma), earth planet. Sci Lett 271:88–100

Lini A, Weissert H, Erba E (1992) The Valanginian carbon isotope event: a first episode of greenhouse climate conditions during the Cretaceous. Terra Nova *4*(3):374–384

Littler K, Robinson SA, Bown PR, Nederbragt AJ, Pancost RD (2011) High Sea-surface temperatures during the early cretaceous epoch. Nat Geosci 4(3):169–172

Lokho K, Tewari VC (2011) Biostratigraphy, Sedimentation and Chemostratigraphy of the Tertiary Neotethys Sediments from the NE Himalaya, India. In Stromatolites: Interaction of Microbes with Sediments (607–630)

Lukeneder A, Suttner TJ, Bertle RJ (2013) New ammonoid taxa from the Lower Cretaceous Giumal Formation of the Tethyan Himalaya (northern India). Palaeontology 56(5):991–1028

MacLeod KG, Huber BT, Berrocoso ÁJ, Wendler I (2013) A stable and hot Turonian without glacial δ18O excursions is indicated by exquisitely preserved Tanzanian foraminifera. Geology 41(10):1083–1086

Mathur NS, Juyal KP (2000) Paleontological evidence for the upheaval history of western Himalaya during the Paleogene. Himal Geol 21(1):109–131

Matsumoto R (1995) Causes of the ^ 1^ 3C anomalies of carbonates and a new paradigm 'Gas-Hydrate Hypothesis'. J Geol Soc Jpn 101:902–924

Matsumoto A, Kobayashi T (1995) K/Ar age determination of late Quaternary volcanic rocks using the "mass fractionation correction procedure": application to the younger on take volcano. Central Japan Chem Geol 125(1-2):123–135

Matsumoto H, Kuroda J, Coccioni R, Frontalini F, Sakai S, Ogawa NO, Ohkouchi N (2020) Marine Os isotopic evidence for multiple volcanic episodes during Cretaceous oceanic anoxic event 1b. Sci Rep 10(1):1–10

McElwain JC, Wade-Murphy J, Hesselbo SP (2005) Changes in carbon dioxide during an oceanic anoxic event linked to intrusion into Gondwana coals. Nature 435(7041):479–482

McInerney FA, Wing SL (2011) The Paleocene-Eocene thermal maximum: a perturbation of carbon cycle, climate, and biosphere with implications for the future. Annu Rev Earth Planet Sci *39*:489–516

Menegatti AP, Weissert H, Brown RS, Tyson RV, Farrimond P, Strasser A, Caron M (1998) High-resolution δ13C stratigraphy through the early Aptian "Livello Selli" of the Alpine Tethys. Paleoceanography 13(5):530–545

Millán MI, Weissert HJ, López-Horgue MA (2014) Expression of the Late Aptian cold snaps and the OAE1b in a highly subsiding carbonate platform (Aralar, northern Spain). Palaeogeogr Palaeoclimatol Palaeoecol 411:167–179

Miller KG, Wright JD, Browning JV (2005) Visions of ice sheets in a greenhouse world. Mar Geol 217(3–4):215–231

Mittal AK, Pandey HC and Singh RR, (2006). Geochemistry of gas seeps from surface shows and wells of the Himalayan foreland basin. In Proceedings of 6th international conference and exposition on petroleum geophysics, Kolkata (235-291).

Moiroud M, Martinez M, Deconinck JF, Monna F, Pellenard P, Riquier L, Company M (2012) High-resolution clay mineralogy as a proxy for orbital tuning: example of the Hauterivian–Barremian transition in the Betic Cordillera (SE Spain). Sediment Geol 282:336–346

Morford JL, Emerson S (1999) The geochemistry of redox sensitive trace metals in sediments. Geochim Cosmochim Acta 63(11-12):1735–1750

Mort H, Jacquat O, Adatte T, Steinmann P, Föllmi K, Matera V, Berner Z, Stüben D (2007) The Cenomanian/Turonian anoxic event at the Bonarelli level in Italy and Spain: enhanced productivity and/or better preservation? Cretac Res 28(4):597–612

Mukherjee S, Misra AA, Calvès G, Nemčok M (2017) Tectonics of the Deccan large igneous province: an introduction. Geol Soc Lond, Spec Publ 445(1):1–9

Muller Karger FE, Varela R, Thunell R, Luerssen R, Hu C, Walsh JJ (2005) The importance of continental margins in the global carbon cycle. Geophys Res Lett 32(1):L01602

Nagendra R, Reddy AN (2017) Major geologic events of the Cauvery Basin, India and their correlation with global signatures–a review. J Palaeogeogr 6(1):69–83

Najarro M, Rosales I, Moreno-Bedmar JA, de Gea GA, Barrón E, Company M, Delanoy G (2011) High-resolution chemo-and biostratigraphic records of the Early Aptian oceanic anoxic

event in Cantabria (N Spain): Palaeoceanographic and palaeoclimatic implications. Palaeogeogr Palaeoclimatol Palaeoecol 299(1-2):137–158
Nathorst AG (1890) Beitrage zur mesozoischen Flora Japans, vol 57. Denks Math-Nat Cl Kaiser, Akad Wiss, Wien, pp 4–60
Navarro-Ramirez JP, Bodin S, Immenhauser A (2016) Ongoing Cenomanian—Turonian heterozoan carbonate production in the neritic settings of Peru. Sediment Geol 331:78–93
Norris RD, Huber BT, Self-Trail J (1999) Synchroneity of the KT oceanic mass extinction and meteorite impact: Blake nose, western North Atlantic. Geology 27(5):419–422
Nozaki T, Suzuki K, Ravizza G, Kimura JI, Chang Q (2012) A method for rapid determination of Re and Os isotope compositions using ID-MC-ICP-MS combined with the sparging method. Geostand Geoanal Res 36(2):131–148
Ohkouchi Y, Inoue Y (2006) Direct production of L (+)-lactic acid from starch and food wastes using Lactobacillus manihotivorans LMG18011. Bioresour Technol 97(13):1554–1562
Ohkouchi N, Kawamura K, Kawahata H, Taira A (1997) Latitudinal distributions of terrestrial biomarkers in the sediments from the Central Pacific. Geochim Cosmochim Acta 61(9):1911–1918
Ohkouchi N, Kashiyama Y, Kuroda J, Ogawa NO, Kitazato H (2006) The importance of diazotrophic cyanobacteria as primary producers during Cretaceous Oceanic Anoxic Event 2. Biogeosciences 3(4):467–478
Ohno S, Kadono T, Kurosawa K, Hamura T, Sakaiya T, Shigemori K, Hironaka Y, Sano T, Watari T, Otani K, Matsui T (2014) Production of sulphate-rich vapour during the Chicxulub impact and implications for ocean acidification. Nat Geosci 7(4):279–282
Owens JD, Lyons TW, Hardisty DS, Lowery CM, Lu Z, Lee B, Jenkyns HC (2017) Patterns of local and global redox variability during the Cenomanian–Turonian Boundary Event (Oceanic Anoxic Event 2) recorded in carbonates and shales from central Italy. Sedimentology 64(1):168–185
Padden M, Weissert H, de Rafelis M (2001) Evidence for late Jurassic release of methane from gas hydrate. Geology 29(3):223–226
Pandey B, Pathak DB (2015) Record of Early Bathonianammonoids from Kachch, India: biostratigraphic and paleobiogeographic implications. J Palaeontol Soc India 60(1):33–44
Pandey B, Pathak DB (2016) The possibility of the Oceanic Anoxic Events (OAEs) study in the Indian marine Jurassic-Cretaceous outcrops. J Geol Soc India 87(3):–261
Pandey B, Pathak DB, Krishna J (2013) Preliminary remarks on new ammonoid collection from freshly exposed succession of the Spiti Formation between Lidang and Giumal, Spiti Valley, Himachal Himalaya, India. Himal Geol 34(2):124–134
Pathak DB (1997) Ammonoid stratigraphy of the Spiti Shale formation in Spiti Himalaya, India. Geol Soc India 50(2):191–200
Pathak DB, Krishna J, Pandey B (2011) Differentiation of the significant Late Valanginian (Early Cretaceous) transgressive event in the Spiti Himalaya, India. J Asian Earth Sci 42(6):1226–1231
Pearce CR, Cohen AS, Coe AL, Burton KW (2008) Molybdenum isotope evidence for global ocean anoxia coupled with perturbations to the carbon cycle during the Early Jurassic. Geology 36(3):231–234
Percival LME, Witt MLI, Mather TA, Hermoso M, Jenkyns HC, Hesselbo SP, Al-Suwaidi AH, Storm MS, Xu W, Ruhl M (2015) Globally enhanced mercury deposition during the end-Pliensbachian extinction and Toarcian OAE: a link to the Karoo–Ferrar Large Igneous Province. Earth Planet Sci Lett 428:267–280
Percival LME, Bond DPG, Rakociński M, Marynowski L, Hood A, Adatte T, Spangenberg JE, Föllmi KB (2020) Phosphorus-cycle disturbances during the Late Devonian anoxic events. Glob Planet Chang 184:103070
Phelps RM, Kerans C, Da-Gama RO, Jeremiah J, Hull D, Loucks RG (2015) Response and recovery of the Comanche carbonate platform surrounding multiple Cretaceous oceanic anoxic events, northern Gulf of Mexico. Cretac Res 54:117–144
Pi DH, Liu CQ, Shields-Zhou GA, Jiang SY (2013) Trace and rare earth element geochemistry of black shale and kerogen in the early Cambrian Niutitang Formation in Guizhou province, South China: constraints for redox environments and origin of metal enrichments. Precambrian Res 225:218–229
Pierazzo E, Hahmann AN, Sloan LC (2003) Chicxulub and climate: radiative perturbations of impact-produced S-bearing gases. Astrobiology 3(1):99–118
Pittet B, Suan G, Lenoir F, Duarte LV, Mattioli E (2014) Carbon isotope evidence for sedimentary discontinuities in the lower Toarcian of the Lusitanian Basin (Portugal): sea level change at the onset of the Oceanic Anoxic Event. Sediment Geol 303:1–14
Poulsen CJ, Barron EJ, Peterson WH, Wilson PA (1999) A reinterpretation of mid-Cretaceous shallow marine temperatures through model-data comparison. Paleoceanography 14(6):679–697
Poulsen CJ, Barron EJ, Arthur MA, Peterson WH (2001) Response of the mid-Cretaceous global oceanic circulation to tectonic and CO2 forcings. Paleoceanography 16(6):576–592
Pratt, L.M., 1985. Isotopic studies of organic matter and carbonate in rocks of the greenhorn marine cycle
Poulton SW, Canfield DE (2011) Ferruginous conditions: a dominant feature of the ocean through Earth's history. Elements 7(2):107–112
Pratt LM and Threlkeld CN, (1984). Stratigraphic significance of 13C/12C ratios in mid-Cretaceous rocks of the Western Interior.
Raiverman V (1979) Stratigraphy and facies distribution, Subathu sediments, Simla Hills, northwestern Himalaya. Geo Survey India Misc Publ 41:111–125
Raiverman V (2002) Foreland sedimentation in Himalayan tectonic regime. In: A relook at the orogenic process. Bishen Singh Mahendra Pal Singh Publication, Dehradun, p 371p
Richiano S (2014) Lower Cretaceous anoxic conditions in the Austral basin, south-western Gondwana, Patagonia Argentina. J S Am Earth Sci 54:37–46
Richter FM, Rowley DB, De Paolo DJ (1992) Sr isotope evolution of seawater: the role of tectonics. Earth Planet Sci Lett 109(1-2):11–23
Rita P, Weis R, Duarte LV and De Baets K, (2020). Taxonomical diversity and palaeobiogeographical affinity of belemnites from the Pliensbachian–Toarcian GSSP (Lusitanian Basin, Portugal). Papers in Palaeontology.
Robinson SA, Heimhofer U, Hesselbo SP, Petrizzo MR (2017) Mesozoic climates and oceans–a tribute to Hugh Jenkyns and Helmut Weissert. Sedimentology 64(1):1–15
Röhl U, Westerhold T, Bralower TJ, and Zachos JC, 2007. On the duration of the Paleocene-Eocene thermal maximum (PETM). Geochem Geophysics Geosyst 8(12).
Royer DL, Pagani M, Beerling DJ (2012) Geobiological constraints on Earth system sensitivity to CO2 during the Cretaceous and Cenozoic. Geobiology 10(4):298–310
Ruebsam W, Mayer B, Schwark L (2019) Cryosphere carbon dynamics control early Toarcian global warming and sea level evolution. Glob Planet Chang 172:440–453
Rumpf CM, Lewis HG, Atkinson PM (2017) Asteroid impact effects and their immediate hazards for human populations. Geophys Res Lett 44(8):3433–3440
Sabatino N, Neri R, Bellanca A, Jenkyns HC, Baudin F, Parisi G, Masetti D (2009) Carbon isotope records of the Early Jurassic (Toarcian) oceanic anoxic event from the Valdorbia (Umbria–Marche Apennines) and Monte Mangart (Julian Alps) sections: palaeoceanographic and stratigraphic implications. Sedimentology 56(5):307–1328
Sabatino N, Coccioni R, Manta DS, Baudin F, Vallefuoco M, Traina A, Sprovieri M (2015) High-resolution chemostratigraphy of the

late Aptian–early Albian oceanic anoxic event (OAE 1b) from the Poggio le Guaine section (Umbria–Marche Basin, central Italy). Palaeogeogr Palaeoclimatol Palaeoecol 426:319–333

Sachse VF, Littke R, Jabour H, Schümann T, Kluth O (2012) Late Cretaceous (late Turonian, Coniacian and Santonian) petroleum source rocks as part of an OAE, Tarfaya Basin, Morocco. Mar Pet Geol 29(1):35–49

Sachsenhofer RF, Popov SV, Akhmetiev MA, Bechtel A, Gratzer R, Groß D, Horsfield B, Rachetti A, Rupprecht B, Schaffar WB, Zaporozhets NI (2017) The type section of the Maikop Group (Oligocene–lower Miocene) at the Belaya River (North Caucasus): depositional environment and hydrocarbon potential. AAPG Bull 101(3):289–319

Sageman BB, Meyers SR, Arthur MA (2006) Orbital time scale and new C-isotope record for Cenomanian-Turonian boundary stratotype. Geology 34(2):125–128

Sahoo SK, Planavsky NJ, Jiang G, Kendall B, Owens JD, Wang X, Shi X, Anbar AD, Lyons TW (2016) Oceanic oxygenation events in the anoxic Ediacaran Ocean. Geobiology 14(5):457–468

Sanchez-Hernandez Y, Florentin JMM (2016) The influence of regional factors in the expression of oceanic anoxic event 1a (OAE1a) in the semi-restricted Organyà Basin, south-Central Pyrenees, Spain. Palaeogeogr Palaeoclimatol Palaeoecol 441:582–598

Sangode SJ, Kumar R (2003) Magnetostratigraphic correlation of the Late Cenozoic fluvial sequences from NW Himalaya, India. Curr Sci:1014–1024

Sangode SJ, Kuma, R and Siddaiah NS, (2005). Magnetic polarity and rock magnetic studies across marine to continental transition (Subathu-Dagshai sequence) in the Himalayan Foreland: Singapore. In Proceedings, Asia Oceania Geosciences meeting (p. 284).

Satpathy KK, Panigrahi S, Mohanty AK, Sahu G, Achary MS, Bramha SN, Padhi RK, Samantara MK, Selvanayagam M, Sarkar SK (2013) Severe oxygen depletion in the shallow regions of the Bay of Bengal off Tamil Nadu Coast. Curr Sci 104(11):1467–1469

Schlanger SO, Jenkyns HC (1976) Cretaceous oceanic anoxic events: causes and consequences. Geologieenmijnbouw 55(3-4):179–184

Schlanger SO, Arthur MA, Jenkyns HC, Scholle PA (1987) The Cenomanian-Turonian oceanic anoxic event, I. Stratigraphy and distribution of organic carbon-rich beds and the marine δ13C excursion. Geol Soc Lond, Spec Publ 26(1):371–399

Scholle PA, Arthur MA (1980) Carbon isotope fluctuations in cretaceous pelagic limestones: potential stratigraphic and petroleum exploration tool. AAPG Bull 64(1):67–87

Schönfeld J, Kuhnt W, Erdem Z, Flögel S, Glock N, Aquit M, Frank M, Holbourn A (2014) Systematics of past changes in ocean ventilation: a comparison of Cretaceous ocean anoxic event 2 and Pleistocene to Holocene oxygen minimum zones. Biogeosci Discuss 11(9):13343–13387

Schopf TJ, Manheim FT (1967) Chemical composition of ectoprocta (Bryozoa). J Paleontol 41:1197–1225

Schouten S, van Kaam-Peters HM, Rijpstra WIC, Schoell M, Damste JSS (2000) Effects of an oceanic anoxic event on the stable carbon isotopic composition of early Toarcian carbon. Am J Sci 300(1):1–22

Schulte P, Alegret L, Arenillas I, Arz JA, Barton PJ, Bown PR, Willumsen PS (2010) The Chicxulub asteroid impact and mass extinction at the Cretaceous-Paleogene boundary. Science 327(5970):1214–1218

Shukolyukov A, Lugmair G (1998) Isotopic evidence for the Cretaceous-Tertiary impactor and its type. Science 282(5390):927–930

Sluijs A, Röhl U, Schouten S, Brumsack HJ, Sangiorgi F, Damsté JSS, Brinkhuis H (2008) Arctic late Paleocene–early Eocene paleoenvironments with special emphasis on the Paleocene-Eocene thermal maximum (Lomonosov ridge, Integrated Ocean drilling program expedition 302). Paleoceanography 23(1)

Singh P (1973) Geology of the Subathu Group of Jammu and Kashmir state. Himal Geol *3*:284–298

Singh BP, Andotra DS (2000) Barrier-lagoon and tidal cycles in Palaeocene to middle Eocene Subathu Formation, NW Himalaya, India. Tertiary Res 20(1/4):65–78

Smit J, Hertogen J (1980) An extraterrestrial event at the Cretaceous–Tertiary boundary. Nature 285(5762):198–200

Song C, Woodcock CE (2003) A regional forest ecosystem carbon budget model: impacts of forest age structure and land use history. Ecol Model 164(1):33–47

Soua M (2014) A review of Jurassic oceanic anoxic events as recorded in the northern margin of Africa, Tunisia. J Geosci Geomatics 2(3):94–106

Soua M (2016) Cretaceous oceanic anoxic events (OAEs) recorded in the northern margin of Africa as possible oil and gas shale potential in Tunisia: an overview. Int Geol Rev 58(3):277–320

Soua M, Chihi H (2014) Optimizing exploration procedure using oceanic anoxic events as new tool for hydrocarbon strategy in Tunisia. In: Gaci S, Hachay O (eds) Chapter Book, in Advances in Data, Methods, Models and Their Applications in Oil/Gas Exploration. Cambridge Scholars Publishing (CSP) Edition, Cambridge, p 55

Soussi M (2003) Nouvelle nomenclature lithostratigraphique «événementielle» pour le Jurassique de la Tunisie atlasique. Geobios 36(6):761–773

SOUSSI M, ISMAIL MHB, M'RABET ALI (1990) Les «black shales» toarciens de Tunisie centrale: témoins d'événement anoxique sur la marge sud téthysienne. Comptes rendus de l'Académie des sciences. Série 2, Mécanique, Physique, Chimie, Sciences de l'univers, Sciences de la Terre 310(5):591–596

Southam JR, Peterson WH, Brass GW (1982) Dynamics of anoxia. Palaeogeogr Palaeoclimatol Palaeoecol 40(1–3):183–198

Speijer R, Wagner T (2002) Sea-level changes and black shales associated with the late Paleocene thermal maximum: organic-geochemical and micropaleontologic evidence from the southern Tethyan margin (Egypt- Israel). Catastrophic events and mass extinctions: Impacts and beyond 356:533–549

Sperling EA, Wolock CJ, Morgan AS, Gill BC, Kunzmann M, Halverson GP, Macdonald FA, Knoll AH, Johnston DT (2015) Statistical analysis of iron geochemical data suggests limited late Proterozoic oxygenation. Nature 523(7561):451–454

Stoll HM, Schrag DP (2000) High-resolution stable isotope records from the upper cretaceous rocks of Italy and Spain: glacial episodes in a greenhouse planet? Geol Soc Am Bull 112(2):308–319

Srikantia SV, Bhargava ON (1998) Geology of Himachal Pradesh: geological society of India. Text Book Series 9:416

Srivastava VK, Casshyap SM (1983) Evolution of pre-Siwalik Tertiary basin of Himachal Himalaya. J Geol Soc India 24(3):134

Suan G, Mattioli E, Pittet B, Mailliot S, Lécuyer C (2008) Evidence for major environmental perturbation prior to and during the Toarcian (Early Jurassic) oceanic anoxic event from the Lusitanian Basin, Portugal. Paleoceanography 23(1):PA1202

Sundaram R, Henderson RA, Ayyasami K, Stilwell JD (2001) A lithostratigraphic revision and palaeoenvironmental assessment of the Cretaceous system exposed in the onshore Cauvery Basin, southern India. Cretac Res 22(6):743–762

Takashima R, Nishi H, Huber BT, Leckie RM (2006) Greenhouse world and the Mesozoic Ocean. Oceanography

Takashima R, Nishi H, Yamanaka T, Tomosugi T, Fernando AG, Tanabe K, Moriya K, Kawabe F, Hayashi K (2011) Prevailing oxic environments in the Pacific Ocean during the mid-Cretaceous oceanic anoxic event 2. Nat Commun 2(1):1–5

Takashima R, Nishi H, Yamanaka T, Hayashi K, Waseda A, Obuse A, Tomosugi T, Deguchi N, Mochizuki S (2010) High-resolution terrestrial carbon isotope and planktic foraminiferal records of the upper Cenomanian to the lower Campanian in the Northwest Pacific. Earth Planet Sci Lett 289(3–4):570–582

Talbi R, Lakhdar R, Smati A, Spiller R, Levey R (2019) Correction to: Aptian–Albian shale oil unconventional system as registration of Cretaceous oceanic anoxic sub-events in the southern Tethys (Bir M'Cherga basin, Tunisia). J Pet Explor Prod Technol 9(2):1023–1024

Tarduno JA, Brinkman DB, Renne PR, Cottrell RD, Scher H, Castillo P (1998) Evidence for extreme climatic warmth from late cretaceous Arctic vertebrates. Science 282(5397):2241–2243

Tewari, A., Hart, M.B. and Watkinson, M.P., 1996. Foraminiferal recovery after the mid-cretaceous oceanic anoxic events (OAEs) in the Cauvery Basin, Southeast India. Geological Society, London, Special Publications, 102(1), 237–244

Tiraboschi D, Erba E, Jenkyns HC (2009) Origin of rhythmic Albian black shales (Piobbico core, central Italy): calcareous nannofossil quantitative and statistical analyses and paleoceanographic reconstructions. Paleoceanography 24(2):PA2222

Tourtelot HA (1979) Black shale—its deposition and diagenesis. Clay Clay Miner 27(5):313–321

Trabucho-Alexandre J, Dirkx R, Veld H, Klaver G, de Boer PL (2012) Toarcian black shales in the Dutch Central Graben: record of energetic, variable depositional conditions during an oceanic anoxic event. J Sediment Res 82(2):104–120

Tsikos H, Jenkyns HC, Walsworth-Bell B, Petrizzo MR, Forster A, Kolonic S, Erba E, Silva IP, Baas M, Wagner T, Damsté JS (2004) Carbon-isotope stratigraphy recorded by the Cenomanian–Turonian oceanic anoxic event: correlation and implications based on three key localities. J Geol Soc 161(4):711–719

Turner JT (2002) Zooplankton fecal pellets, marine snow and sinking phytoplankton blooms. Aquat Microb Ecol 27(1):57–102

Uveges BT, Junium CK, Scholz CA, Fulton JM (2020) Chemocline collapse in Lake Kivu as an analogue for nitrogen cycling during oceanic anoxic events. Earth Planet Sci Lett 548:116459

Valle B, Dal'Bó PF, Mendes M, Favoreto J, Rigueti AL, Borghi L, Silva R Jr (2019) The expression of the oceanic anoxic event 2 (OAE2) in the northeast of Brazil (Sergipe-Alagoas Basin). Palaeogeogr Palaeoclimatol Palaeoecol 529:12–23

van Breugel Y, Schouten S, Tsikos H, Erba E, Price GD, Sinninghe Damsté JS (2007) Synchronous negative carbon isotope shifts in marine and terrestrial biomarkers at the onset of the early Aptian oceanic anoxic event 1a: evidence for the release of 13C-depleted carbon into the atmosphere. Paleoceanography 22(1)

Van Cappellen P, Ingall ED (1994) Benthic phosphorus regeneration, net primary production, and ocean anoxia: a model of the coupled marine biogeochemical cycles of carbon and phosphorus. Paleoceanography 9(5):677–692

Van Helmond NA, Sluijs A, Reichart GJ, SinningheDamsté JS, Slomp CP, Brinkhuis H (2014) A perturbed hydrological cycle during oceanic anoxic event 2. Geology 42(2):123–126

Voigt S, Gale AS, Voigt T (2006) Sea-level change, carbon cycling and palaeoclimate during the late Cenomanian of Northwest Europe; an integrated palaeoenvironmental analysis. Cretac Res 27(6):836–858

Voigt S, Erbacher J, Mutterlose J, Weiss W, Westerhold T, Wiese F, Wilmsen M, Wonik T (2008) The Cenomanian-Turonian of the Wunstorf section-(North Germany): global stratigraphic reference section and new orbital time scale for oceanic anoxic event 2. Newsl Stratigr 43(1):65

Wagner T, Sinninghe Damsté JS, Hofmann P, Beckmann B (2004) Euxinia and primary production in late cretaceous eastern equatorial Atlantic surface waters fostered orbitally driven formation of marine black shales. Paleoceanography 19(3)

Wang CS, Hu XM, Jansa L, Wan XQ, Tao R (2001) The Cenomanian–Turonian anoxic event in southern Tibet. Cretac Res 22(4):481–490

Wang J, Chen D, Yan D, Wei H, Xiang L (2012) Evolution from an anoxic to oxic deep ocean during the Ediacaran–Cambrian transition and implications for bioradiation. Chem Geol 306:129–138

Wang T, Li G, Aitchison JC, Ding L, Sheng J (2019a) Evolution of mid-Cretaceous radiolarians in response to oceanic anoxic events in the eastern Tethys (southern Tibet, China). Palaeogeogr Palaeoclimatol Palaeoecol 536:109369

Wang M, Wilkins RW, Song G, Zhang L, Xu X, Li Z, Chen G (2015) Geochemical and geological characteristics of the Es3L lacustrine shale in the Bonan sag, Bohai Bay basin, China. Int J Coal Geol 138:16–29

Wang X, Collett TS, Lee MW, Yang S, Guo Y, Wu S (2014) Geological controls on the occurrence of gas hydrate from core, downhole log, and seismic data in the Shenhu area, South China Sea. Mar Geol 357:272–292

Wang Y, Xu S, Hao F, Lu Y, Shu Z, Lu Y (2019b) Geochemical and petrographic characteristics of Wufeng-Longmaxi shales, Jiaoshiba area, southwest China: implications for organic matter differential accumulation. Mar Pet Geol 102:138–154

Weissert H, Erba E (2004) Volcanism, CO2 and palaeoclimate: a Late Jurassic–Early Cretaceous carbon and oxygen isotope record. J Geol Soc 161(4):695–702

Wendler I, Wendler J, Gräfe KU, Lehmann J, Willems H (2009) Turonian to Santonian carbon isotope data from the Tethys Himalaya, southern Tibet. Cretac Res 30(4):961–979

Wignall P (2005) The link between large igneous province eruptions and mass extinctions. Elements 1(5):293–297

Wignall PB, Hallam A (1992) Anoxia as a cause of the Permian/Triassic mass extinction: facies evidence from northern Italy and the western United States. Palaeogeogr Palaeoclimatol Palaeoecol 93(1–2):21–46

Wignall PB, Hallam A, Newton RJ, Sha JG, Reeves E, Mattioli E, Crowley S (2006) An eastern Tethyan (Tibetan) record of the early Jurassic (Toarcian) mass extinction event. Geobiology 4(3):179–190

de Wit MJ, Ghosh JG, de Villiers S, Rakotosolofo N, Alexander J, Tripathi A, Looy C (2002) Multiple organic carbon isotope reversals across the Permo-Triassic boundary of terrestrial Gondwana sequences: clues to extinction patterns and delayed ecosystem recovery. The Journal of Geology 110(2):227–240

Witts JD, Newton RJ, Mills BJ, Wignall PB, Bottrell SH, Hall JL, Francis JE, Crame JA (2018) The impact of the cretaceous–Paleogene (K–Pg) mass extinction event on the global sulfur cycle: evidence from Seymour Island, Antarctica. Geochim Cosmochim Acta 230:17–45

Wolbach WS, Gilmour I, Anders E, Orth CJ, Brooks RR (1988) Global fire at the Cretaceous–Tertiary boundary. Nature 334(6184):665–669

Wynne AB (1872) Memoir on the Geology of Kutch, to accompany the map compiled by AB Wynne and F Fedden during the season 1867–1869 Geological Survey of India. Memoir 19(2):1–269

Wyrtki K (1962) The subsurface water masses in the western South Pacific Ocean. Mar Freshw Res 13(1):18–47

Yan D, Wang H, Fu Q, Chen Z, He J, Gao Z (2015) Geochemical characteristics in the Longmaxi Formation (Early Silurian) of South China: implications for organic matter accumulation. Mar Pet Geol 65:290–301

Zachos JC, Röhl U, Schellenberg SA, Sluijs A, Hodell DA, Kelly DC, Kroon D (2005) Rapid acidification of the ocean during the Paleocene-Eocene thermal maximum. Science 308(5728):1611–1615

Zeebe RE, Zachos JC, Dickens GR (2009) Carbon dioxide forcing alone insufficient to explain Palaeocene-Eocene thermal maximum warming. Nat Geosci 2(8):576